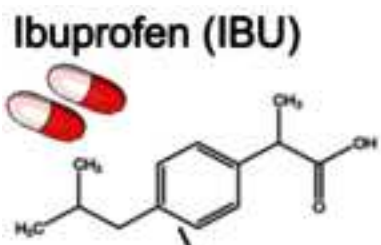


Journal of Hazardous Materials

Exposure of the seagrass *Cymodocea nodosa* to seawater contaminated by the pharmaceutical ibuprofen: an analysis of the potential impact at multiple plant levels --Manuscript Draft--

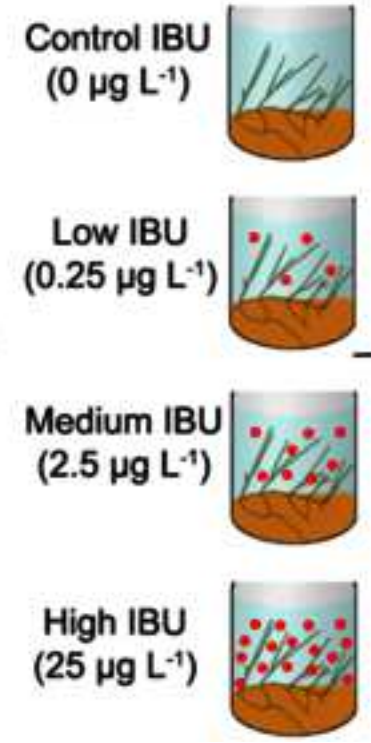
Manuscript Number:	
Article Type:	Research Paper
Keywords:	non-steroidal anti-inflammatory drug (NSAID); oxidative stress; photosynthetic efficiency; secondary metabolites; resilience
Corresponding Author:	Elena Balestri, Ph.D. University of Pisa Pisa, ITALY
First Author:	Virginia Menicagli
Order of Authors:	Virginia Menicagli Monica Ruffini Castiglione Emily Cioni Carmelina Spanò Elena Balestri, Ph.D. Marinella De Leo Stefania Bottega Carlo Sorce Claudio Lardicci
Abstract:	<p>Pharmaceuticals such as ibuprofen entering marine environments are of great concern due to their increasing consumption and impact on aquatic organisms. Very little is still known about the toxicity of ibuprofen to marine photosynthetic organisms, and no information is available for foundation species like seagrasses, which are declining globally to anthropogenic factors. Here, the effects of short-term exposure (12 days) of the seagrass <i>Cymodocea nodosa</i> to environmentally realistic IBU concentrations (0.25-2.5-25 $\mu\text{g L}^{-1}$) at multiple levels (plant growth, oxidative status, photosynthetic efficiency, and secondary metabolites content) were assessed in mesocosm. Chemical analyses to detect the presence of ibuprofen and its products in seawater medium and plants were also performed. Ibuprofen was undetected in plants and did not affect their growth but caused oxidative damage and altered antioxidant enzyme activity. At the highest concentration, ibuprofen also increased photosynthetic pigment content and damaged the photosynthetic machinery, particularly PSII and its donor side. Moreover, it halved phenolic acid and flavonoid content while increased rutin, gallic acid, and coumaric acid. These findings suggest that <i>C. nodosa</i> could tolerate short-term ibuprofen exposure through stress mitigation strategies, but they raise concern about the potential risk of a prolonged exposure on plant resilience and on associated ecosystems.</p>
Suggested Reviewers:	Durgesh Tripathi dktripathiau@gmail.com Eduardo Gusmão Pereira egpereira@ufv.br

Pharmaceuticals, such as ibuprofen, are considered as emerging contaminants due to their potential adverse effects on marine wildlife. This study is the first documenting the effects of environmentally relevant concentrations of ibuprofen detected in the Mediterranean Sea on marine plants (seagrasses), which play fundamental ecological roles, at multiple levels. It shows that short-term exposure of *Cymodocea nodosa* plants to ibuprofen, especially to the highest concentration, caused oxidative stress and photosynthetic machinery damage. These findings provide valuable insights for assessing the potential risk posed by a prolonged exposure to this pollutant to seagrasses and their resilience against environmental stressors.



Seagrass meadows

Laboratory experiment

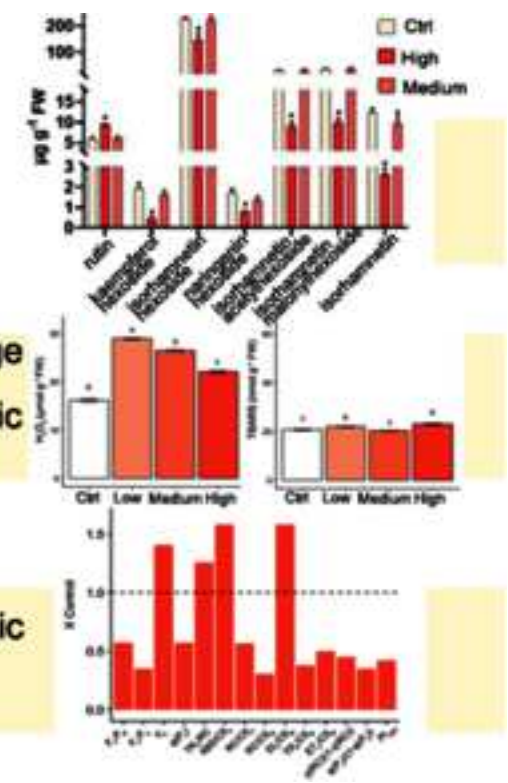


Cymodocea nodosa
exposure to IBU

-affected secondary metabolite production

-caused oxidative damage
-increased photosynthetic pigment content

-damaged photosynthetic machinery



- Effects of seawater contamination by IBU on *Cymodocea nodosa* plants was assessed.
- IBU was detected in the growth medium but not inside plant tissues.
- IBU altered secondary metabolite production and caused oxidative stress in plants.
- IBU damaged photosynthetic machinery, especially PSII, at high concentration.
- Prolonged exposure to high IBU amounts may reduce seagrass resilience.

1 **Exposure of the seagrass *Cymodocea nodosa* to seawater contaminated by the pharmaceutical**
2 **Ibuprofen: an analysis of the potential impact at multiple plant levels**

3
4
5 3
6
7 4 Virginia Menicagli^{a,1}, Monica Ruffini Castiglione^{a,b,c,1}, Emily Cioni^{d,1}, Carmelina Spanò^{a,c,1}, Elena
8
9 5 Balestri^{a,b,*}, Marinella De Leo^{b,d}, Stefania Bottega^a, Carlo Sorce^{a,c,1}, Claudio Lardicci^{b,c,e,1}

10
11 6
12
13 7 ^a Department of Biology, University of Pisa, via L. Ghini 13, 56126 Pisa, Italy

14
15
16 8 ^b Center for Instrument Sharing University of Pisa (CISUP), University of Pisa, Lungarno Pacinotti
17
18 9 43-44, 56126 Pisa, Italy

19
20
21 10 ^c Center for Climate Change Impact, University of Pisa, Via Del Borghetto 80, 56124 Pisa, Italy

22
23 11 ^d Department of Pharmacy, University of Pisa, Via Bonanno Pisano 6, 56126 Pisa, Italy

24
25 12 ^e Department of Earth Sciences, University of Pisa, via S. Maria 53, 56126 Pisa, Italy

26
27
28 13
29
30 14 ¹ These authors equally contributed.

31
32
33 15 *Corresponding author elena.balestri@unipi.it, University of Pisa, Department of Biology, Via
34
35 16 Derna 1, 56126 Pisa, Italy

36
37
38 17

39
40 18

41
42 19

43
44
45 20

46
47 21

48
49
50 22

51
52 23

53
54
55 24

56
57 25

58
59 26

60
61
62
63
64
65

27 **Abstract**

1
28 Pharmaceuticals such as ibuprofen entering marine environments are of great concern due to their
3
4
29 increasing consumption and impact on aquatic organisms. Very little is still known about the
6
30 toxicity of ibuprofen to marine photosynthetic organisms, and no information is available for
8
9
31 foundation species like seagrasses, which are declining globally to anthropogenic factors. Here, the
10
11
12 effects of short-term exposure (12 days) of the seagrass *Cymodocea nodosa* to environmentally
13
14
15 realistic IBU concentrations (0.25-2.5-25 $\mu\text{g L}^{-1}$) at multiple levels (plant growth, oxidative status,
16
17
18 photosynthetic efficiency, and secondary metabolites content) were assessed in mesocosm.
19
20
21
22
23
24
25
26
27
28
29
30
31
32
33
34
35
36
37
38
39
40
41
42
43
44
45
46
47
48
49
50
51
52
53
54
55
56
57
58
59
60
61
62
63
64
65

45 **Environmental implication statement**

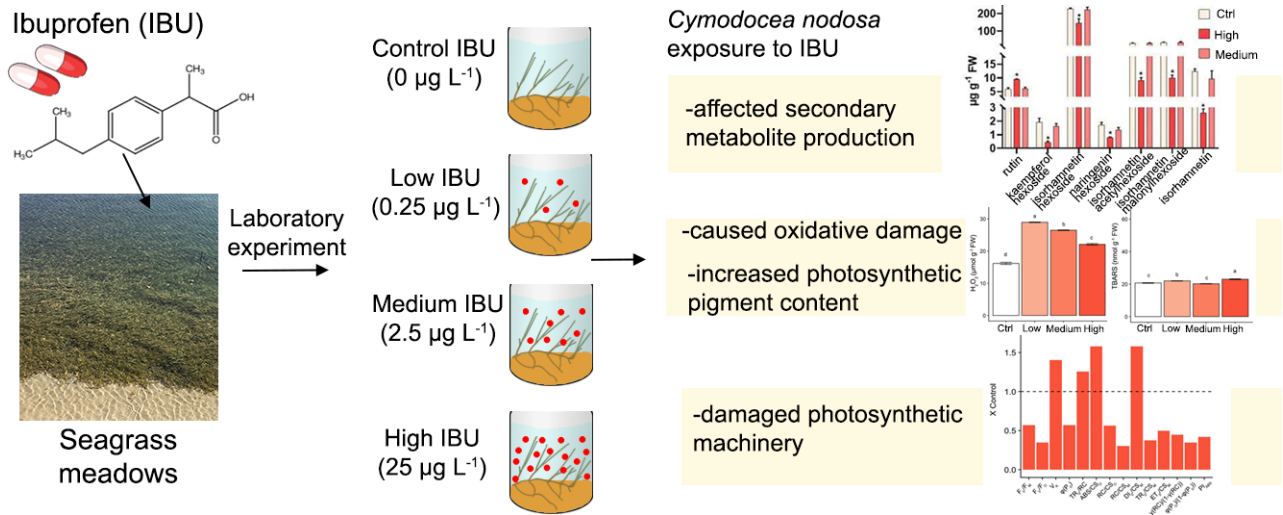
46
47
48
49
50
51
52
53
54
55
56
57
58
59
60
61
62
63
64
65

insights for assessing the potential risk posed by a prolonged exposure to this pollutant to seagrasses and their resilience against environmental stressors.

Keywords

non-steroidal anti-inflammatory drug (NSAID); oxidative stress; photosynthetic efficiency; secondary metabolites; resilience

Graphical abstract



Highlights

- Effects of seawater contamination by IBU on *Cymodocea nodosa* plants was assessed.
- IBU was detected in the growth medium but not inside plant tissues.
- IBU altered secondary metabolite production and caused oxidative stress in plants.
- IBU damaged photosynthetic machinery, especially PSII, at high concentration.
- Prolonged exposure to high IBU amounts may reduce seagrass resilience.

78 **1 Introduction**

1
2
3 79 The presence of active pharmaceutical ingredients (APIs) as well as of their metabolites and
4
5 80 degradation products in marine environments is an issue of increasing global concern due to their
6
7 81 potential adverse effects, both in isolation and in combination with other global-change-related
8
9 82 stressors, on aquatic organisms (Ankley et al., 2007; Branchet et al., 2021; Ibanez et al., 2021;
10
11 83 Blasco and Trombini, 2023; Kock et al., 2023). These chemicals enter the marine environment
12
13 84 continuously through various point and nonpoint sources (e.g., urban and hospital wastewater
14
15 85 treatment plant effluents, water bodies, animal husbandry and aquacultures) where they are present
16
17 86 at concentrations in the range of ng L^{-1} - $\mu\text{g L}^{-1}$ due to their systemic use and lack of effective
18
19 87 removal technologies (Madikizela et al., 2020; Alfonso-Muniozguren et al., 2021; Blasco and
20
21 88 Trombini, 2023). Up to 600 pharmaceutical substances have been detected in seawater and marine
22
23 89 sediments (Adeleye et al., 2022; Blasco and Trombini, 2023), and some of them have been included
24
25 90 in the European Water Framework Directive “Watch-list” as potentially harmful (EU, 2013) even if
26
27 91 a strict and comprehensive regulation is still lacking. Some pharmaceuticals have also been found in
28
29 92 marine animals, like mollusks, crustaceans, and fish (Álvarez-Muñoz et al., 2015; Maranhão et al.,
30
31 93 2015; Świacka et al., 2019), as well as in macrophytes, such as macroalgae and seagrasses
32
33 94 (Álvarez-Muñoz et al., 2015; Ali et al., 2018; Long et al., 2023). However, current knowledge on
34
35 95 the toxicity of these chemicals to marine organisms is limited and mostly referred to few specific
36
37 96 animal taxa and target species (Gonzales-Rey and Bebianno, 2011; Matozzo et al., 2012; de Orte et
38
39 97 al., 2013; Mezzelani et al., 2018; Almeida et al., 2020; Silva et al., 2020; Mezzelani and Regoli,
40
41 98 2022; Świacka et al., 2022).

42
43
44 99 The few available information on the effects of pharmaceuticals on marine macrophytes as well
45
46 100 as on their uptake mechanisms concerns macroalgae (Wiklund et al., 2011; Oskarsson et al., 2012;
47
48 101 Ali et al., 2018). No study has dealt so far with the effects of these substances on marine
49
50 102 angiosperms (seagrasses) to our knowledge. These plants are exposed to a wide range of chemicals,
51
52 103 including sunscreen UV filters contained in personal care products and pharmaceuticals, since they
53
54
55
56
57
58
59
60
61
62
63
64
65

104 grow in shallow coastal areas even in proximity to urban and industrial effluents (Lewis and
1
105 Devereux, 2009; García-Marquez et al., 2023; Li et al., 2023; Long et al., 2023). Some species like
3
106 *Zostera marina* L., *Cymodocea nodosa* (Ucria) Ascherson, and *Posidonia oceanica* L. Delile are
4
6 recommended as biological indicators for marine environmental quality assessment due to their
107
8 capacity to bioaccumulate chemicals present in sediments and water column (Montefalcone, 2009;
9
108 Marbà et al., 2013). However, seagrass populations are declining globally due to climate change
10
11
109 and anthropogenic disturbances resulting in the loss of important ecological functions and multiple
12
13 services they provide to humans (Boudouresque et al., 2009; Barbier et al., 2011; McMahon et al.,
14
15
110 2022). Thus, assessing whether the occurrence of pollutants of emerging concern like
16
17
111 pharmaceuticals in marine habitats may pose a further threat to these plants is crucial and will help
18
19
112 in developing more effective seagrass conservation strategies and management interventions.
20
21
22
23
24
25

26
115 One of the most frequently detected pharmaceuticals in coastal surface seawaters is Ibuprofen
27
28 (hereafter IBU). This compound, belonging to the therapeutic group of non-steroidal anti-
29
30 inflammatory drugs (NSAIDs), has an estimated annual global consumption of over 10,000 metric
31
32 tons and has attracted much attention in the last years because of its use during the COVID-19
33
34
35 pandemic (Wilton and Brant, 2013; Almeida et al., 2020; Wang et al., 2021; Ferreira et al., 2023).
36
37
38
39
40 IBU can be introduced in aquatic environments both in its original form (i.e., the parent compound
41
42 2-(4-Isobutylphenyl) propionic acid) and in its metabolites generated after consumption by humans
43
44 or animals (Rainsford, 2009). IBU has been found in European and Mediterranean coastal seawater
45
46
47 at average concentrations of 1.5-2.5 $\mu\text{g L}^{-1}$ (Togola and Budzinski, 2008; Loos et al., 2013;
48
49
124 Mezzelani et al., 2018; Madikizela et al., 2020), and it is considered as a pseudo-persistent pollutant
50
51
52 that can undergo degradation (half-life in freshwater is of 12 days; Ding et al., 2017) and
53
54
55 phototransformation resulting in the formation of many intermediates (Vione et al., 2011). Lower
56
57 concentrations (range of ng L^{-1}) have been observed in marine sediments probably due to the low
58
128 sorption capacity of sediments for IBU at pH around 8 (Blasco and Trombini, 2023).
59
60
61
62
63
64
65

129 Studies on the effects of the seawater contamination by IBU on marine microalgae have shown
1
130 that the exposure of the target species, the diatom *Pheodactylum tricornutum* Bohlin, to
3
131 concentrations (100-300 $\mu\text{g L}^{-1}$) higher than those detected in natural marine environments resulted
6
132 in a reduction of the growth rate, oxidative stress, and changes in the photosynthetic pathway
8
133 functioning (Silva et al., 2020). Instead, no effect was found in the macroalga *Fucus vesiculosus* L.,
10
134 following the exposure to much higher IBU concentrations (up to 10,000 $\mu\text{g L}^{-1}$; Wiklund et al.,
13
135 2011; Oskarsson et al., 2012). Studies on the impact of IBU on macrophytes inhabiting other
16
136 aquatic environments, like saltmarshes, rivers, and lakes (Brain et al., 2004; Pomati et al., 2004; Iori
18
137 et al., 2013; Pietrini et al., 2015; Li et al., 2016; Di Baccio et al., 2017; He et al., 2017) have shown
20
138 that some species, including *Typha angustifolia* L., *Phragmites australis* (Cav.) Trin. ex Steud. and
23
139 *Salix alba* L., can metabolize and degrade this compound via detoxifying reactions involving
25
140 specific enzymes (e.g., cytochrome P450 monooxygenase, glycosyltransferase, and glutathione-S
27
141 transferase) resulting in no adverse effects on plants (Li et al., 2016; He et al., 2017). However, a
30
142 growth inhibition in *Lemna minor* L. and a growth stimulation in *Lemna gibba* L. was detected
32
143 upon the exposure to a 1000 $\mu\text{g L}^{-1}$ IBU concentration (Pomati et al., 2004; Pietrini et al., 2015).
35

144 The aim of this study was to evaluate the potential impact of seawater contamination by IBU on
37
145 the performance of seagrasses using *C. nodosa* as a model. This species was selected because of its
40
146 occurrence in shallow coastal areas often in proximity to freshwater inputs, fast growth rate and
42
147 responsiveness to environmental changes and contaminants (e.g., metals and plastics; Cancemi et
45
148 al., 2002; Agostini et al., 2003; Borum et al., 2004; Malea et al., 2018; Menicagli et al., 2021,
47
149 2022). Specifically, through a multidisciplinary approach involving plant morphological traits and
49
150 growth measurements, qualitative and quantitative secondary metabolites analyses, oxidative stress
52
151 evaluation (i.e., oxidative stress markers, antioxidant enzyme activity, and histochemical assay), and
54
152 photosynthetic efficiency assessment, the effects of a short-term exposure (12 days) of plants to
57
153 environmentally realistic IBU concentrations for the Mediterranean basin were explored.
59
60
61
62
63
64
65

155 **2 Materials and Methods**

156 *2.1 Chemicals*

157 Standard IBU (CAS number 15687-27-1) was purchased from Sigma Aldrich, Germany (purity \geq
158 98%). Physico-chemical properties of IBU are reported in Table S1. A stock solution of IBU (10 mg
159 L⁻¹ in ethanol) was prepared and stored at room temperature in laboratory. Ultra High-Performance
160 Liquid Chromatography (UHPLC) grade methanol, water, formic acid, and the standards rutin (\geq
161 98% purity) and chicoric acid (\geq 95% purity) were purchased from Merck KGaA (Darmstadt,
162 Germany). Catechin standard was previously isolated and characterized by 1D- and 2D-NMR, and
163 HR-MS techniques in authors laboratory from other plant extracts. All the analytical grade solvents
164 were acquired from VWR (Milano, Italy).

166 *2.2 Plant material and experimental set-up*

167 In May 2023, *C. nodosa* plagiotropic rhizome fragments were harvested in a shallow site (0.5 m)
168 located in the Ligurian Sea (Italy, 43°22'55.66"N, 10°26'7.05"E). Fragments were transported to the
169 laboratory and cut into experimental plant units of homogenous size (7.05 ± 0.08 cm, mean \pm SE,
170 $n=60$, rhizome length; 4.18 ± 0.09 shoot number; 0.71 ± 0.43 root number). Each plant unit was
171 gently placed into a mesocosm consisting of a glass culture vessel (0.5 L) containing natural
172 seawater (NSW, pH = 8.13 ± 0.03 , practical salinity unit = 38.03 ± 0.03) and a layer (3 cm) of silica
173 sand (grain size 0.5–1 mm, density 1.6 g mL^{-1} , and less than 0.01% of organic matter content),
174 previously washed and sterilized. NSW was provided by INVE Aquaculture Research Center of
175 Rosignano Solvay and filtered as described in Menicagli et al. (2022) before its use. A commercial
176 NPK fertilizer (Cifo, 20-10-10, 0.44 g L^{-1}) was added in each mesocosm to sustain plant growth. All
177 mesocosms were placed in a culture chamber at environmental conditions like those experienced by
178 plants in their natural habitat at the time of collection (20 °C, 12/12h light/dark regime,
179 photosynthetic photon flux density $110\text{-}150 \mu\text{mol m}^{-2} \text{ s}^{-1}$) and left undisturbed for 7 days for plant
180 acclimatization. At the end of the acclimatization, the NSW in each mesocosm was renewed, and

181 each mesocosm was assigned to one of the four nominal IBU seawater concentrations (0 $\mu\text{g L}^{-1}$ or
1
2
182 Control, 0.25 $\mu\text{g L}^{-1}$ or Low, 2.5 $\mu\text{g L}^{-1}$ or Medium, 25 $\mu\text{g L}^{-1}$ or High) mimicking those detected in
3
4
183 European coastal seawaters (average concentration of 1.5-2.5 $\mu\text{g L}^{-1}$; Togola and Budzinski, 2008;
5
6
184 Loos et al., 2013; Mezzelani et al., 2018; Madikizela et al., 2020). Such concentrations were
7
8
9
185 achieved by dissolving appropriate aliquots of the IBU stock solution in the NSW added to
10
11
186 mesocosms. There were 15 replicates for each treatment (60 plants in total). Before assigning plants
12
13
187 to the IBU treatments, their morphological variables (number of shoots, average number of leaves
14
15
16
188 per shoot, length of the longest leaf on the apical shoot, and rhizome length) were recorded.
17
18
19
189 Additional mesocosms (12) containing sand, NSW and IBU at the same four concentrations as
20
21
22
190 described above but without the plant unit inside were also prepared (3 replicates per each
23
24
25
191 treatment) and used as blank. Plants were maintained under the same culture conditions as those
26
27
28
192 experienced during the acclimatization period. The NSW was renewed after 7 days from the
29
30
31
193 experiment beginning and spiked with aliquots of the IBU stock solution according to the nominal
32
33
34
194 concentrations. Plants were daily inspected, and the mesocosms were reallocated spatially to avoid
35
36
37
195 position effects. At the end of the experiment (after 12 days of exposure to IBU), ten plants per each
38
39
40
196 treatment were collected and used for morphological trait and growth measurements (section 2.3),
41
42
43
197 detection of IBU and qualitative and quantitative analyses of specialized plant metabolites (sections
44
45
46
198 2.4 and 2.5), and oxidative stress evaluation (i.e., oxidative stress markers, antioxidant enzyme
47
48
49
199 activity, and histochemical assay; from section 2.6 to 2.8). The remaining five plants per each
50
51
52
200 treatment were used for measurements of the effect of IBU exposure on the photosynthetic
53
54
55
201 efficiency (section 2.9). NSW samples were also collected from mesocosms and analyzed to detect
56
57
58
202 IBU and its main metabolites (section 2.4 and 2.5).
59
60
61
62
63
64
65

203 204 *2.3 Plant morphological traits and growth measurements*

205 At the end of the experiment, the number of survived plants in each treatment was determined and
206 their morphological variables were measured. The net change in shoot number for each plant was

207 calculated as the difference between the number of newly produced shoots and that of dead shoots
1
208 within the experimental exposure period. The net change in leaf number was calculated as the
2
3
4
209 difference between the number of newly produced leaves and that of detached leaves averaged
5
6
210 across all the standing shoots present on each plant within the experimental exposure period. Leaf
7
8
211 (or rhizome) elongation was calculated as the difference between the final length and the initial
9
10
212 length of the longest leaf on the apical shoot (or the rhizome) over the initial length and expressed
11
12
13
213 as a percentage.
14
15

214 16 17 18 19 2.4 Preparation of NSW and plant extract samples for chemical analyses 20

21 Before assigning plants to IBU treatments, NSW samples (50 mL) were collected from mesocosms
22
23
24 containing only NSW (negative control) or IBU at high, medium, and low concentration. IBU-
25
26
27 supplemented NSW samples were also collected at the end of the experiment from mesocosms
28
29 containing *C. nodosa* plants as well as from blank mesocosms (without *C. nodosa* plants). All NSW
30
31
220 samples were evaporated under vacuum (Buchi Rotavapor[®], Milano, Italy) and the residues were
32
33
221 partitioned with *n*-BuOH/H₂O (1:2 v/v) to remove salts and centrifuged for 5 min at 2710 × g. The
34
35
222 *n*-butanol fractions were subjected to vacuum drying and finally dissolved in 100 μL of methanol for
36
37
223 liquid chromatography (LC) coupled to mass spectrometry (MS) analyses. The whole *C. nodosa*
38
39
224 plants (1 g), grown in mesocosms without IBU (i.e., control) and containing the different IBU
40
41
42 concentrations, were subjected to extraction with 5 mL of methanol for 15 min by ultrasonic bath
43
225 LBS2 (Falc Instruments s.r.l., Treviglio, Italy) and finally centrifuged for 5 min at 2710 × g. The
44
45
226 supernatants were transferred into vials to be injected into the LC-MS system.
46
47
48
227
49
50

228 51 52 53 2.5 Ibuprofen-targeted and quali-quantitative liquid chromatography-high-resolution mass 54 55 230 spectrometry (LC-HR-MS) analyses of plant specialized metabolites 56 57

231 The solutions (5 μL) obtained from NSW and plant samples were injected into an UHPLC coupled
58
59
60
232 with a diode array detector (DAD) and a high resolution (HR) Q Exactive Plus Orbitrap MS, equipped
61
62
63
64
65

233 with an electrospray ionization (ESI) source and a hybrid quadrupole analyzer (Thermo Fischer
1 Scientific Inc., Bremen, Germany). The chromatographic runs were performed by using a Kinetex[®]
234 Biphenyl C-18 column (2.1 x 100 mm, 2.6 μm) equipped with a Security GuardTM Ultra Cartridge
235 (Phenomenex, Bologna, Italy) at a flow rate of 0.5 mL min⁻¹. The autosampler and the column oven
236 were maintained at a temperature of 4 °C and 35 °C, respectively. As a mobile phase, a mixture of
237 HCOOH/H₂O 0.1% v/v (solvent A) and HCOOH/MeOH 0.1% v/v (solvent B) was chosen and a
238 linear gradient was used, increasing from 5 to 80% B in 20 min. The ESI-HR mass spectra were
239 recorded in negative and positive ion modes, operating in Parallel Reaction Monitoring (PRM) for
240 IBU detection. Standard solutions of IBU were used as reference standards, with IBU detected both
241 in negative ($[\text{M}-\text{H}]^-$ at m/z 205.1228; $[\text{M}+\text{H}]^+$ at m/z 207.1376, Figure S1). For the analysis of
242 specialized metabolites, a scan range of m/z 135-2000 was applied, recording MS both in full (70000
243 resolution, 220 ms maximum injection time) and data dependent-MS/MS scan (17500 resolution, 60
244 ms maximum injection time). UV data were recorded in a range of 200–600 nm, using 254, 280 and
245 325 nm as preferential channels. Nebulization voltage of 3500 V, capillary temperature of 300 °C,
246 sheath gas (N₂) 20 arbitrary units, auxiliary gas (N₂) 3 arbitrary units, HCD (Higher-energy C-trap
247 dissociation) of 18 eV were applied as ionization settings (Cioni et al., 2024). IBU and its main
248 metabolites (hydroxyibuprofen, dihydroxyibuprofen, ibuprofen glucoside, and carboxyibuprofen),
249 possibly produced by phase I and II metabolism of plants (He et al., 2017), were compared among
250 samples by considering the areas of the extracted ion peaks from the chromatograms obtained by LC-
251 MS analyses. The specialized metabolites in the plant extracts were quantified by using three pure
252 external standards such as chicoric acid, rutin and catechin. Triplicate solutions of chicoric acid and
253 rutin were prepared in a concentration range of 1.95-62.5 $\mu\text{g mL}^{-1}$, obtaining calibration curves with
254 a good linearity over the entire range and a correlation coefficient (R^2) equal to 0.999 and 0.998,
255 respectively. Catechin calibration curve was prepared in a concentration range of 12.5-100 $\mu\text{g mL}^{-1}$,
256 showing $R^2 = 0.992$. Xcalibur 4.1 software (Thermo Fisher Scientific Inc., Bremen, Germany) was
257

258 used to process acquired chromatographic profiles and MSⁿ (n = 1, 2 levels) spectra.–Results were
1 expressed as $\mu\text{g g}^{-1}$ of FW \pm standard deviation (SD).
259

260
261 *2.6 Oxidative stress markers: hydrogen peroxide, thiobarbituric acid reactive substances and*
262 *histochemical assay*

263 The determination of hydrogen peroxide (H₂O₂) and thiobarbituric acid reactive substances
264 (TBARS) in plant samples was performed according to Jana and Choudhuri (1982) and Spanò et al.
265 (2017), respectively. To measure H₂O₂ concentrations, leaves and rhizomes were homogenized in
266 50 mM phosphate buffer (pH 6.5), centrifuged, and the supernatant was mixed with 0.1% titanium
267 chloride in 20% (v/v) H₂SO₄, and the absorbance was read at 410 nm. The concentration of H₂O₂
268 was determined by employing a standard curve and then expressed in micromoles per gram of fresh
269 weight ($\mu\text{mol g}^{-1}$ FW). TBARS concentration was determined by measuring absorbance at 532 nm
270 after subtracting non-specific absorbance at 600 nm, and quantified as nmol g^{-1} FW, following
271 homogenization and extraction of plant material.

272 Leaves of similar size and length from five randomly chosen plants per treatment were isolated
273 and divided into tip and mid-leaf segments. H₂O₂ was detected histochemically by dipping leaf
274 portions in a staining solution containing 1 mg mL⁻¹ DAB at pH 3.8, followed by vacuum
275 infiltration for 20 min (Daudi and O'Brien, 2012). After that, the samples were left overnight in the
276 same solution, then treated with 96% ethanol for 60 min at 65 °C, and finally examined under a
277 light microscope to assess the presence of brown precipitates. In situ determination of lipid
278 peroxidation was conducted using Schiff's reagent (Yamamoto et al., 2001) (VWR Chemicals
279 BDH), which binds to free aldehyde groups, serving as a qualitative indicator of lipid peroxidation.
280 Leaf segments were incubated with the dye for 60 min at room temperature, followed by bleaching
281 in 96% ethanol for 60 min at 65 °C. The samples were then examined under a light microscope to
282 evaluate the development of a purple coloration. Histochemical analyses were performed using a
283 Leitz Diaplan microscope, with images captured using a Leica DFC 420 camera.

284 Cross sections of rhizomes from the same five plants were prepared using a hand microtome.
1
285 Detection of H₂O₂ within the rhizome slices was conducted following the method outlined by
2
3
4
286 Giorgetti et al. (2019), utilizing Amplex UltraRed Reagent (Life Technologies, USA). Following
5
6
287 staining, the slices were mounted in glycerol and examined using a fluorescence microscope with
7
8
288 excitation/emission wavelengths of 568ex/681em nm. Lipid peroxidation levels were assessed using
9
10
289 a fluorescence microscope by observing the change in fluorescence emission peak from red to green
11
12
290 after staining with the BODIPY 581/591 C11 probe (Life Technologies, USA), as described by
13
14
291 Spanò et al. (2020). Microscope evaluation involved acquiring both green (485ex/510em nm) and
15
16
292 red fluorescence (581ex/591em nm) signals simultaneously and merging the two images.
17
18
293 Fluorescence microscope analysis was carried out using a Leica DMLB microscope equipped with
19
20
294 the appropriate excitation/emission filters, along with a Leica DFC7000 T camera.
21
22
23
24
25
26
27
28

296 *2.7 Extraction and determination of the activity of antioxidant enzymes in plants*

29
30

297 Antioxidant enzymes were extracted from plant samples in 100 mM potassium phosphate buffer
31
32
298 (pH 7.5), following the procedure outlined in Spanò et al. (2013). The activity of ascorbate
33
34
299 peroxidase (APX, EC 1.11.1.11) was measured according to Nakano and Asada (1981), monitoring
35
36
300 the decrease in absorbance at 290 nm (extinction coefficient of 2.8 mM⁻¹ cm⁻¹) as ascorbate was
37
38
301 oxidized. A correction for the non-enzymatic oxidation of ascorbate by hydrogen peroxide (blank)
39
40
302 was applied. Catalase (CAT, EC 1.11.1.6) activity was determined following the method described
41
42
303 by Aebi (1984) and calculated using the extinction coefficient of 39.4 mM⁻¹ cm⁻¹. A blank
43
44
304 containing only the enzymatic solution was prepared. Guaiacol peroxidase (POX, EC 1.11.1.7)
45
46
305 activity was determined according to the method described by Arezki et al. (2001), using 1%
47
48
306 guaiacol as substrate and measuring guaiacol oxidation by H₂O₂ at 470 nm (extinction coefficient of
49
50
307 26.6 mM⁻¹ cm⁻¹), with one unit oxidizing 1.0 μmol guaiacol per minute. Superoxide dismutase
51
52
308 (SOD, EC 1.15.1.1) activity was determined as per Beyer and Fridovich (1987), with slight
53
54
309 modifications as detailed in Spanò et al. (2016). One SOD unit was defined as the amount required
55
56
57
58
59
60
61
62
63
64
65

310 to inhibit by 50% the photoreduction of nitroblue tetrazolium, measured spectrophotometrically at
1
311 550 nm. All enzymatic activities were assessed at 25°C and expressed as units per milligram of
3
4
312 protein (U mg⁻¹ protein). Protein quantification was conducted following the method of Bradford
5
6
313 (1976), utilizing bovine serum albumin (BSA) as a standard.
8

314 10 11 315 *2.8 Extraction and determination of plant photosynthetic pigments* 13

14
316 Leaf chlorophylls (a, b, and total) and carotenoids were extracted following the method outlined by
15
16
317 Hassanzadeh et al. (2009). In summary, leaves were homogenized in 80% acetone, and the extracts
18
19
318 were then centrifuged for 10 min at 6000 g at 4°C. After collecting the supernatants, the pellets
20
21
319 were resuspended and re-extracted with 80% acetone until they became colourless. The combined
22
23
320 supernatants were analyzed using a spectrophotometer at wavelengths of 645 nm, 663 nm, and 470
25
26
321 nm. Pigment contents were calculated using the formula developed by Lichtenthaler (1987) and
27
28
322 expressed as milligrams per gram of fresh weight (mg g⁻¹ FW).
30

31 323 32 33 324 *2.9 Chlorophyll a Fluorescence Transient Kinetics* 35

36
325 The analysis of PSII fluorescence was carried out to determine the effects of IBU on the total
37
38
326 functional efficiency of plants. A Handy PEA fluorometer (Hansatech Instruments Ltd., Pentney,
40
41
327 King's Lynn, UK) was used to record fluorescence at four times: just before the treatment with IBU
42
43
328 (T0), and one, five and twelve days following the treatment (T1, T5 and T12, respectively). Plants
44
45
329 were acclimated to darkness for 30 min, then they were withdrawn from water and quickly blotted
47
48
330 on paper to eliminate the excess of water. Two leaf clips were applied to each plant (one clip for
49
50
331 each shoot) and the two values recorded on each plant were averaged to yield a single replicate:
52
53
332 consequently, five replicates were available for each treatment. After having recorded chlorophyll
54
55
333 fluorescence, plants were put back in the water. All operations were carried out in darkness, with
57
58
334 the aid of a dim, diffuse light which was used only during the preparation of the plants. To avoid
59
60
335 interferences on fluorescence kinetic data resulting from exposure to such light source,
62
63
64
65

336 measurements were taken after the leaves had been with the clips applied for 4 min: based on
1
337 preliminary tests, this time lapse had proven to be sufficient for the purpose. Chlorophyll a
3
4
338 fluorescence (ChlF) was measured after the darkened areas were exposed for 1 s to 3500 μmol
5
6
339 photons $\text{m}^{-2} \text{s}^{-1}$ (peak wavelength of 650 nm). Data were processed by PEA Plus software
8
9
340 (Hansatech Instruments Ltd.), which carried out the analysis of the fast fluorescence kinetics, or JIP
10
11
341 test (Stirbet et al., 2018). Each treatment's records were averaged to produce a single value, which
13
14
342 was subsequently handled as a separate replicate. The JIP test parameters were computed using F_0 ,
15
16
343 F_J , F_I , and F_M in addition to the ChlF values that were obtained at 50 μs , 100 μs , and 300 μs
18
19
344 (Paunov et al., 2018). Table S2 contains a list of the parameters.
20
21
22
23

346 2.10 Statistical analyses

26
347 The effects of the exposure of *C. nodosa* plants to IBU contaminated seawater on morphological
27
28
348 traits and growth measurements, specialized metabolites, oxidative stress markers, antioxidant
30
31
349 enzyme activity, photosynthetic pigments, and photosynthetic efficiency were assessed through a
32
33
350 one-way analysis of variance (ANOVA, “GAD” package, Sandrini-Neto and Camargo, 2014).
35
36
351 Before performing ANOVAs, the normality and homoscedasticity of data were assessed by
37
38
352 Shapiro–Wilk test and Cochran C test, respectively. Since some data did not meet ANOVA
40
41
353 assumptions, they were analyzed by a Kruskal-Wallis test. In case of a significant effect, a
42
43
354 Dunnett’s test was conducted to compare the amount of detected specialized metabolite between
44
45
355 IBU treated plants and control ones while Tukey HSD post-hoc tests (or Dunn test for APX in
47
48
356 leaves) were carried out on other response variables. The statistical analyses were performed in R
49
50
357 environment (version 3.5.2; R Core Team, 2018) and by JMP[®] Pro 16.0.0 (SAS Institute Inc., Cary,
52
53
358 NC, USA) software.
54
55

360 3 Results and Discussion

361 3.1 Plant morphological traits and growth measurements

362 No difference in shoot number, average number of leaves per shoot, length of the longest leaf, and
1
363 rhizome length of plants attributed to different IBU concentrations was detected at the beginning of
3
4
364 the experiment (i.e., before the exposure to IBU; Table S3, Figure S2). At the end of the
6
365 experiment, statistical analyses did not detect any significant effects of IBU on plant morphological
8
9
366 and growth traits (Table S4, Figure 1, S3). These results agree with previous studies reporting no
10
11
367 effect on the growth of the marine macroalga *F. vesiculosus* (Wiklund et al., 2011; Oskarsson et al.,
13
14
368 2012), the marine diatom *P. tricornutum* (Silva et al., 2020) as well as on freshwater plants like *L.*
15
16
369 *gibba*, *L. minor*, and *S. alba* (Pomati et al., 2004; Iori et al., 2013; Di Baccio et al., 2017) after their
18
19
370 exposure to IBU concentrations within the range of those used in the present study.
20
21

22
23

372 3.2 Profiling Ibuprofen and plant specialized metabolites

25

26
373 LC-MS analyses revealed the presence of linearly decreasing concentrations of IBU in the NSW
28
29
374 medium supplemented with high, medium, and low concentrations of IBU (positive controls) and
30
31
375 the absence of IBU in the NSW samples (negative controls)(data not shown). The IBU-
32
33
376 supplemented NSW collected at the end of the experiment from mesocosms containing or not *C.*
35
36
377 *nodosa* plants showed IBU levels in agreement with the positive controls at all tested
37
38
378 concentrations. The presence of IBU or its metabolites in the *C. nodosa* extracts was not detected,
40
41
379 suggesting that this compound was not internalized by plants or alternatively that it was under the
42
43
380 detection limit of the analytical method.
44

45
381 Furthermore, to investigate if the presence of IBU influenced the production of specialized
47
48
382 metabolites, a quali-quantitative chemical analysis of specialized metabolites in extracts prepared
49
50
383 from *C. nodosa* plants exposed to medium and high IBU concentrations was carried out by LC-MS
52
53
384 techniques. This work stands out as a crucial contribution to the elucidation of the chemical
54
55
385 composition of *C. nodosa* plant, as there are few other investigations in the literature (Grignon-
57
58
386 Dubois and Rezzonico, 2013; Milović et al., 2019). The chromatographic profiles of control plants
59
60
387 compared to treated ones are shown in Figure 2. A total of 39 compounds (Table S5) were
61
62
63
64
65

388 tentatively identified by comparing their retention times (t_R), HR full mass spectra, and
1
389 fragmentation patterns with data reported in the literature, considering an accepted mass error <5
2
390 ppm on the experimental molecular formula. A tricarboxylic acid, 23 phenolic acids and
3
4
5
6
391 derivatives, 13 flavonoids, and 2 dihydrochalcones were found. Citric acid (**1**) displayed the loss of
7
8
9
392 CO₂ and two water molecules (base ion peak at m/z 111.00) (Fernández-Fernández et al., 2010).
10
11
393 Among phenolic acids, gallic acid (**2**), hydroxybenzoic acid (**3**, [M – H][–] at m/z 137.0239),
12
13
394 coumaric acid (**17**, [M – H][–] at m/z 163.0396), dihydrocoumaric acid (**18**, [M – H][–] at m/z
14
15
395 165.0553) and ferulic acid (**23**, [M – H][–] at m/z 193.0503) exhibited all the loss of a CO₂ molecule
16
17
18
396 (-44 u) (Astudillo-Pascual et al., 2021). Compound **5** was identified as dihydroxybenzoic acid
19
20
21
397 hexoside, showing the loss of a monosaccharide portion (-162 u). Compounds **4**, **6** and **11** were not
22
23
24
398 completely annotated, but the presence of base ion peaks at m/z 137.02, 151.04, 165.06,
25
26
399 respectively, suggested that these molecules are hydroxybenzoic, hydroxymethylbenzoic,
27
28
400 dihydrocoumaric acid derivatives (Ostrowski et al., 2014). Coumaroyl hexoside isomers (**12** and **13**)
29
30
401 showed a diagnostic product ion at m/z 163.04 (-162 u). Feruloyltartaric acid (**14**), feruloylhexoside
31
32
402 (**16**) and feruloylmalic acid (**24**) displayed ferulic acid as a product ion at m/z 193.05. Caftaric acid
33
34
403 isomers were attributed to peaks **7** and **21** by considering the product ion at m/z 149.01 (tartaroyl
35
36
37
404 residue). Similarly, coutaric acid (**10**) and dicoumaroyltartaric acid (**32**) exhibited a tartaroyl
38
39
40
405 product ion (Carazzone et al., 2013; Milović et al., 2019). Coumaroylmalic acid (**19**) showed a base
41
42
406 ion peak at m/z 163.04 due to the cleavage of an ester bond with malic acid. Chicoric acid (**20**), a
43
44
45
407 valuable compound previously found in *C. nodosa* plant (Grignon-Dubois and Rezzonico, 2013),
46
47
408 showed the consecutive loss of two caffeoyl residues (product ions at m/z 311.04 and 149.01) and
48
49
50
509 tartaric acid as a product ion (peak at m/z 179.03). Compounds **26** and **31** differed from caftaric acid
51
52
53
510 only for the presence of an additional coumaroyl and feruloyl moieties, respectively. Similarly,
54
55
56
511 compound **38** showed an additional feruloyl unit, compared to feruloyltartaric acid (**14**). Since roots
57
58
59
512 were included in the extraction of the *C. nodosa* plants, also catechins and derivatives, typically
60
61
62
63
64
65
513 found in barks, were detected in the extracts. Catechin and epicatechin (**8** and **15**) showed the

414 product ion at m/z 245.08 (Navarro et al., 2018). Procyanidin B-type dimer (9) displayed diagnostic
1
415 ions at m/z 451.10, 425.09 and 287.05 as previously reported by Cioni et al. (2024). Among
3
416 flavonoids, rutin (22), quercetin hexoside (25), quercetin malonylhexoside (27) exhibited the
4
5
6
417 presence in the mass spectra of the same base ion peak at m/z 300.03 (aglycon portion) (López-
8
9
418 Fernández et al., 2020; Navarro-Hoyos et al., 2021). Furthermore, MS² analysis revealed the
10
11
419 presence of kaempferol hexoside (28) and naringenin hexoside (33) both displaying the loss of a
13
14
420 hexose unit (Sánchez-Rabameda et al., 2003). Isorhamnetin rutinoside (29), isorhamnetin hexoside
15
16
421 (30), isorhamnetin acetylhexoside (35), and isorhamnetin malonylhexoside (36) all exhibited a base
18
19
422 ion peak at m/z 315.04 in the MS/MS, corresponding to the aglycon portion isorhamnetin, also
20
21
423 detected in the extracts (39). Finally, the metabolomic analysis revealed the presence of two
22
23
424 dihydrochalcones, phloretin (37) and its glucoside form phlorizin (34), exhibiting ESI-MS² peaks in
25
26
425 agreement with data reported in the literature (Lijia et al., 2014).
27
28

426 The quantitative analysis showed a significant change in the production of some specialized
30
31
427 metabolites among both phenolic acids and flavonoids, especially in the extracts from plants
32
33
428 exposed to high concentrations of IBU compared to the control ones. In general, total phenolic acids
35
36
429 and flavonoids were almost halved in the plants treated with high IBU concentrations ($480 \pm 61 \mu\text{g}$
37
38
430 $\text{g}^{-1} \text{FW} \pm \text{SD}$), compared to the control ones ($821 \pm 52 \mu\text{g g}^{-1} \text{FW} \pm \text{SD}$) (Table S6). The specialized
40
41
431 metabolites reported in Figure 3 significantly decreased in their content in the plants treated with
42
43
432 high/medium concentrations of IBU, except for rutin, gallic acid, coumaric acid, and
45
46
433 dihydrocoumaric acid derivative which, instead, showed an increase. Finally, catechin, epicatechin
47
48
434 and procyanidin B-type dimer showed a not significantly change under IBU treatment. These
49
50
435 results, showing that high IBU concentrations affect the production of specialized metabolites, are
52
53
436 consistent with previous studies (Ismail et al., 2015; Gorni et al., 2022; Zhang et al., 2022), where
54
55
437 abiotic stress conditions induce plants to modulate the expression of genes involved in the
57
58
438 biosynthetic pathways of some specialized metabolites, and in particular, to overproduce the ones
59
60
61
62
63
64
65

439 known for the antioxidant properties capable of increasing the plant stress tolerance, such as rutin,
440 gallic acid and coumaric acid.

441
442 *3.3 Oxidative stress evaluation, antioxidant enzyme activity and photosynthetic pigments*

443 Data in the literature support that IBU, like other pharmaceutical pollutants, can induce an oxidative
444 burst in the terrestrial crop *Vigna unguiculata* (L.) Walp. (Wijaya et al., 2020), with the
445 overproduction of ROS, among which H₂O₂, that plays a key role in oxidative stress, and can cause
446 damage to cell structure and macromolecules. In the present study, no significant difference in H₂O₂
447 rhizome concentration among control and treatments was recorded, except at the medium
448 concentration in which the lowest value was detected (Table S7; Figure 4a). In our study, the lack
449 of an increase in H₂O₂ levels in *C. nodosa* aligns with the results observed in *V. unguiculata*
450 (Wijaya et al., 2020). In this latter, indeed, no significant increases in the concentration of this
451 signaling molecule was found at a concentration of 400 ppm.

452 Applying the histochemical approach, which allows direct visualization of H₂O₂ in the rhizome,
453 the staining linked to the fluorescent probe used (Amplex Ultrared) showed specific localization
454 patterns within the organ tissues (Figure 5). The red signal was uniformly distributed in the control,
455 slightly more intensely colouring the epidermis and cortical vascular bundles (Figure 5a). In plants
456 exposed to the low IBU concentration, the pattern extended to part of the compact outer cortical
457 tissue (Figure 5c), which in plants attributed to the medium and high concentration became overall
458 intensely positive to the probe (Figure 5e,g). Furthermore, in plants exposed to the medium IBU
459 concentration, but especially in those at the highest one, even the inner cortical tissue with large air
460 spaces was positive for the dye, including the central stele (Figure 5e,g). These histochemical
461 findings indicate that IBU, while not changing the overall H₂O₂ levels, can influence tissue-specific
462 reactions depending on the concentration.

463 Biochemical results obtained in leaves were quite different, as all the plants exposed to IBU had
464 levels of H₂O₂ significantly higher than control ones, the highest content being recorded at the low

465 concentration, with values that progressively decreased at medium and high concentration (Table
1
466 S7; Figure 4b). The present findings highlight the importance of using narrow concentration ranges
3
4
467 as the response can change even with small changes in concentration, which may not be detected
5
6
468 when these ranges are very broad (Wijaya et al., 2020). These trends also underline that the
8
9
469 response to environmental stimuli depends on the organ, being the leaves more sensitive than the
10
11
470 rhizome. Indeed, histochemical results also confirm an intense H₂O₂-dependent colorimetric
13
14
471 response in the leaf, which was obtained with the DAB dye (Figure 6), whose signal was detectable
15
16
472 by light microscopy, to avoid interferences with the red autofluorescence of chlorophyll. All the
18
19
473 leaves of IBU exposed plants were more intensely dark-brown stained in respect to the control, both
20
21
474 in the tips and in the mid-leaf segments, with no specific staining pattern, demonstrating a general
23
24
475 disturbance, slightly more prominent in the middle portion of the leaf of plants exposed to the
25
26
476 medium and high IBU concentration (Figure 6f,h). These findings in histochemistry support the
27
28
477 previous biochemical evidence, confirming that the leaf is more sensitive to IBU than the rhizome.
30
31
478 This higher sensitivity may be related to the direct contact of leaves with the drug within water
32
33
479 column.

480 Oxidative damage estimated as TBARS, indirect measurement of membrane damage, had in
37
38
481 rhizome similar values in all treatments (Table S7; Figure 4c), while its histochemical
39
40
482 determination (Figure 5) has shown specific differences as for H₂O₂: in control plants, only the
42
43
483 epidermis was positive for Bodipy staining, while in plants exposed to low and medium IBU
44
45
484 concentration, the staining was also present in the vascular cortical bundles (Figure 5d, f) and
47
48
485 extended to the internal cortical tissues in those at the high concentration (Figure 5h). For the
49
50
486 leaves, the quantitatively determined oxidative damage was higher at the maximum IBU
52
53
487 concentration, the lowest values characterized controls and plants under the medium concentration
54
55
488 of this pharmaceutical, while those exposed at the low concentration had intermediate contents
57
58
489 (Table S7; Figure 4d) in accordance with results obtained histochemically with the Schiff reagent
59
60
490 (Figure 7). Overall, both biochemical and histochemical data sustain that IBU can induce oxidative
61
62
63
64
65

491 damage even when administered at concentrations environmentally relevant. These results are
1
492 consistent with previous data on the diatom *P. tricornutum*, in which an overall increment in lipid
3
493 peroxidation, estimated as TBARS, in an IBU concentration-dependent manner was recorded (Silva
4
5
6
494 et al., 2020).

495 To counteract oxidative injury, plants have evolved a complex antioxidant machinery, including
9
10
11
496 enzymes such as POX, CAT, APX and SOD. With the only exception of SOD, differences in the
12
13
14
497 activity of antioxidant enzymes were recorded, with increase and/or decrease in the two organs
15
16
498 (Table 1a, S7). Present results differ from those obtained under comparable IBU concentrations in
17
18
499 *P. tricornutum* (Silva et al., 2020), in which significant differences were detected for SOD activity
19
20
21
500 and not for APX and CAT activities. In fact, in rhizome APX activity had the highest value at the
22
23
501 low and medium IBU concentration and it had a lower value at the high concentration and in
24
25
502 control samples (Table 1a, S7). POX and CAT activities progressively decreased and increased
26
27
28
503 respectively in plants exposed to the low and high IBU concentration with intermediate values at
29
30
31
504 medium concentration (Table 1a, S7). Slight increase in activity of APX (for plants at the low and
32
33
505 medium concentration) and CAT (for plants at the high concentration) seemed able to limit
34
35
506 oxidative stress. In leaves, while CAT and SOD activities were similar in all treatments, APX and
36
37
38
507 POX activities progressively decreased from the low to the high concentration (Table 1a, S7). In
39
40
508 plants treated with the high IBU concentration, the highest oxidative damage in terms of TBARS
41
42
43
509 coincided with the lowest activities of POX and APX.
44
45

510 Among pigments (Table 1b), significant differences were recorded in the concentration of
46
47
511 chlorophyll b, that was significantly higher in plants exposed to the high IBU concentration (Table
48
49
50
512 S7). This was reflected in the content of total chlorophyll that reached the highest value just in this
51
52
53
513 treatment, with intermediate values at medium concentration. The increase in chlorophyll b is of
54
55
514 particular interest, and it could be an attempt of plants to increase the ability to harvest light in the
56
57
515 restrictive conditions induced by stress, and that nevertheless could increase the probability of
58
59
60
516 photoinhibition (Bascañán-Godoy et al., 2012). Considering this, the significant increase in
61
62
63
64
65

517 carotenoids found in plants exposed to the highest concentration, might be an attempt to protect the
1
518 photosynthetic apparatus (Figure S4). In contrast with the present results, under 1 mg L⁻¹ IBU,
3
519 Pietrini et al. (2015), showed no difference in pigment concentrations between the IBU-treated
4
6
520 materials and the controls in *L. gibba*.

521
10
11
522 *3.4 Chlorophyll a Fluorescence Transient Kinetics*

523 Some pollutants have been found to negatively affect photosynthetic parameters that may be used
14
15
524 as markers of phytotoxicity (Iori et al., 2013). In the present work, the analysis of the fast
16
18
525 fluorescence kinetics was carried out to determine the effects of IBU on the photosynthetic
19
20
21
526 efficiency of *C. nodosa*. Data interpretation is based primarily on Krüger et al. (2014), Paunov et al.
22
23
527 (2018), Tsimilli-Michael (2020) and Zagorchev et al. (2021).

528 The parameters of the JIP test at T0 and T1 did not demonstrate any significant difference among
26
27
529 control and treated plants, therefore these data are not shown. Similarly, exposure to the low and
28
29
30
530 medium IBU concentrations did not induce significant changes at any time. Conversely, the effects
31
32
33
531 of IBU at the highest concentration were evident after 5 days and 12 days of exposure (at T5 and
34
35
532 T12). At T5, plants exposed to the highest concentration displayed numerous differences from the
36
37
38
533 controls (Figure 8), with some parameters that demonstrated the onset of a state of stress, whereas
39
40
534 others apparently suggested that IBU also produced some positive effect. These parameters are
41
42
43
535 reported in the following graphs as xControl values, that is, as ratios between treatment and control
44
45
536 data, clustered according to their magnitudes, to facilitate comparisons. The dashed lines indicate
46
47
48
537 the value 1, i.e., the Control, to which all the values of treated plants are referred (Figure 8).

538 At T5 (Figure 8a), in treated *C. nodosa* plants the stress was detectable in the greater dissipation
50
51
52
539 of chlorophyll excitation energy (higher F₀/F_M and DI₀/RC) and lower efficiency of the Hill
53
54
55
540 reaction (F_V/F_O), perhaps a consequence of damage to the oxygen evolving complex, OEC (Gupta,
56
57
541 2020); also the parameter $\phi(P_0)/(1-\phi(P_0))$, functionally analogous to F_V/F_O, was lower in plants
58
59
60
542 exposed to the highest IBU concentration. Perhaps the most obvious symptom of the onset of the
61
62
63
64
65

543 stress was the decrease in the number of active reaction centers per cross section of excited PSII
1
544 (RC/CS_M). In addition, each of the RCs that were still active at the time of fluorescence recording
3
545 experienced a decrease in the maximum quantum yield of the primary photochemistry of PSII
4
546 (F_V/F_M and φ(P₀)). Apparent positive effects of IBU could be inferred from the following
6
547 parameters, that were higher in treated plants: ET₀/RC (electron flux from Q_A⁻ to Q_B per active
8
548 RC), ψ(E₀) (efficiency with which an electron trapped by PSII is transferred from Q_A⁻ to Q_B, ψ(R₀)
10
549 (efficiency with which an electron trapped by PSII is transferred to PSI end acceptors), δ(R₀)
11
550 (efficiency with which an electron is transferred from PQH₂ to PSI end acceptors), RE₀/RC
12
551 (electron flux transferred from PQH₂ to PSI end acceptors per active RC), ψ(E₀)/(1-ψ(E₀))
13
552 (contribution of intersystem electron transport to the overall performance of photosynthesis light
14
553 reactions), and δ(R₀)/(1-δ(R₀)) (contribution of electron transport from Q_B to PSI end acceptors to
15
554 the overall performance of photosynthesis light reactions). Altogether, these parameters
16
555 demonstrate that the energy flux in the intersystem and on the acceptor side of PSI, as well as the
17
556 efficiencies with which the electrons were transferred through these sections of the transport chain,
18
557 were higher following the exposure to IBU. This may be the consequence of increased
19
558 photosynthetic cyclic and pseudocyclic electron flow around PSI (CEF and PEF, respectively),
20
559 which are known to help generating a ΔpH across the thylakoid membranes that enhances non-
21
560 radiative dissipation of light energy (Makino et al., 2002): the high dissipation of excitation energy
22
561 (F₀/F_M and DI₀/RC) recorded in treated individuals substantiates this interpretation. A further
23
562 beneficial effect arising from an enhanced PEF may be the increase of antioxidant enzymes activity
24
563 and of antioxidant molecules concentration (Cheng et al., 2021). Nevertheless, these responses were
25
564 not sufficient to counteract the advancement of the stress.
26
565

566 After 12 days of exposure (i.e., T12), the JIP test highlighted a worsening of the photochemical
567 efficiency, with several parameters that were significantly different between control and treated *C.*
568 *nodosa* (Figure 8b, c). As occurred at T5, the IBU treatment induced a greater dissipation of
chlorophyll excitation energy: however, at T12 this was demonstrated not only by higher values of

569 F_0/F_M and DI_0/RC (Figure 8c), but also by higher DI_0/CS_O (Figure 8c) and DI_0/CS_M (Figure 8b). In
1
570 particular, DI_0/RC shows how RCs were struggling with the management of absorbed light energy,
3
571 which was dissipated at high rates. It is reasonable to assume that during the few days (twelve)
6
572 elapsed from the start of the treatment, the plants could not regulate light energy absorption through
8
573 the adjustment of the size of their antennas. This is suggested by the values of ABS/CS_O (Figure 8b)
10
574 and ABS/CS_M : the former parameter was about 1.5 xControl, while the latter did not differ from the
13
575 Control. This agrees with the concentration of chlorophyll b, which was higher in IBU treated
15
576 plants than in control ones at T12. Consequently, photon absorption under IBU treatment went on
18
577 without changes, while operation of RCs was severely hindered. The value of ABS/RC , in fact
20
578 (Figure 8c), was primarily the consequence of the inactivation of a large number of RCs. This
23
579 process is confirmed by RC/CS_O and RC/CS_M (Figure 8b), that in treated *C. nodosa* were half, or
25
580 even less, compared to the control. In addition, $\gamma(RC)/(1-\gamma(RC))$ (Figure 8b) was lower in treated
27
581 leaves, showing that IBU also caused the decrease of the number of active RCs per chlorophyll
30
582 molecule of PSII antenna. The residual active RCs showed a lower maximum quantum yield of the
32
583 primary photochemistry of PSII (F_V/F_M and $\phi(P_0)$; Figure 8b). The OECs appeared to be damaged
35
584 more severely than at T5, because in addition to lower F_V/F_O and $\phi(P_0)/(1-\phi(P_0))$, the JIP test
37
585 yielded also a higher V_K (Figure 8b). The decrease in the number of active RCs explains why some
40
586 parameters (S_M , N , $S_M/t(F_M)$ and TR_0/RC) seemed to indicate that IBU also had some positive
42
587 effect. S_M was higher in plants exposed to the highest IBU concentration (Figure 8c), which meant
45
588 more electron transporters per chain: however, S_M represents the number of transporters that were
47
589 reduced between O and P per active RC, so if the number of active RCs declined, the value of S_M
49
590 increased. Also, N was higher in treated plants (Figure 8c), probably for the same reason: with
52
591 fewer active RCs, the number of times they were reduced between O and P increased. Similarly, the
54
592 higher $S_M/t(F_M)$ (higher average excitation energy of the open RCs between O and P) of IBU-
57
593 treated individuals (Figure 8c) can be explained by the low number of RCs remained active, which
59
594 were therefore burdened with more energy. Another data that is only apparently positive is the
62
63
64
65

595 higher TR_0/RC of the plants exposed to the highest IBU concentration (Figure 8b): this too can be
1
596 attributed to the low number of RCs remained active, each of which trapped more excitons because
3
4
597 they were subjected to a strong flux of photon energy from the antennas, whose dimensions had not
5
6
598 changed from the start of the experiment. In fact, both the trapping of excitons (TR_0/CS_M) and the
8
9
599 electron flux from Q_A^- to Q_B per cross section of excited PSII (ET_0/CS_M) (Figure 8b) were lower in
10
11
600 treated *C. nodosa*, because of the decreased energy input into the photosynthetic transport chain
13
14
601 consequent to the inactivation of many RCs. All the negative effects described so far can also
15
16
602 explain the lower PI_{ABS} (performance index of energy conservation of photons absorbed until Q_B
18
19
603 reduction) of the treated individuals (Figure 8b). Another set of parameters demonstrates that the
20
21
604 energy flux in the final part of the photosynthetic electron transport chain was greater in IBU-
22
23
605 treated plants. This cannot be attributed, as it was in the case of the previously described
25
26
606 parameters, to the decline of the number of active RCs. Although the higher RE_0/RC (Figure 8c) of
27
28
607 treated plants might indeed depend on the lower number of active RCs, some parameters clearly
30
31
608 suggest another explanation. Among these, RE_0/CS_O and ϕR_0 (Figure 8c), i.e., the electron flux
32
33
609 from PQH_2 to PSI end acceptors per cross section of excited PSII and the quantum yield of electron
35
36
610 transport to PSI end acceptors, respectively, were higher in treated *C. nodosa*, demonstrating that a
37
38
611 greater energy flux actually took place in the last section of the electron transport chain. In
40
41
612 agreement with these data and with this interpretation, also $\psi(E_0)/(1-\psi(E_0))$ and $\delta(R_0)/(1-\delta(R_0))$
42
43
613 (Figure 8c), respectively the contribution of intersystem electron transport and of electron transport
44
45
614 from Q_B to PSI end acceptors to the overall performance of the light reactions of photosynthesis,
47
48
615 were higher in treated plants. As already pointed out for T5, this greater energy flux in the final
49
50
616 section of the transport chain may be the consequence of increased photosynthetic CEF and PEF
52
53
617 around PSI.
54

55
618 Overall, exposure to $25 \mu\text{g L}^{-1}$ IBU caused severe damage to the photosynthetic machinery of *C.*
57
619 *nodosa*, in a relatively short time. The first symptoms of physiological stress were detected by the
59
60
620 JIP test already at T5, but they could have been occurred even earlier. The main targets of the toxic
62
63
64
65

621 action of IBU were PSII and its donor side, with damages to RCs and to OECs, while antenna
1
622 complexes did not seem to be affected. An attempt of exposed plants to protect PSII from the
3
623 impact of IBU might be the increase of carotenoids concentration, which was detected at T12. In
4
624 treated plants, the flux of energy through the intersystem, PSI and its acceptor side was enhanced,
6
625 probably because of the greater activity of CEF and PEF, a response with which the plant aimed at
9
626 accelerating energy dissipation (Figure S4). Apparently, PEF did not strengthen antioxidant
11
627 defenses because the related enzymes showed only a decline of APX and POX activity in plants
14
628 exposed to the highest IBU concentration, that also underwent oxidative damage, as revealed by the
16
629 levels of their TBARS.
18
20

21
630 Less severe impacts have been observed on hydroponically grown *S. alba* plants, treated with 3
23
631 or 30 mg L⁻¹ IBU for two weeks (Iori et al., 2013). Plants showed a decline of Φ PSII, F_v/F_m , qP
25
632 and increased NPQ, that were attributed to the impairment of PSII RCs and the overexcitation of the
26
633 photochemical system, which might had led to the generation of reactive radicals, responsible for
28
634 the damage to PSII components. The aquatic plant *L. gibba* exhibited a notable resistance to IBU.
31
635 Plants treated for 8 days with 20, 200 or 1000 μ g L⁻¹ IBU did not show any changes in the values of
33
636 F_v/F_m , Φ PSII, qP and ETR and the lowest concentration even increased Φ PSII (Di Baccio et al.,
35
637 2017). It is worth noting that, in most cases, both *S. alba* and *L. gibba* had been exposed to IBU
38
638 concentrations that were higher than those applied in the present work on *C. nodosa*, whose
40
639 sensitivity and vulnerability to IBU and, probably, to its metabolites are far greater than in the
42
640 above-mentioned species. The disturbance of the functioning of photosynthetic machinery could be
43
641 considered as an early warning signal of the exposure to IBU. Thus, the analysis of the fast
45
642 fluorescence kinetics may be effective in monitoring the impact of this pollutant on *C. nodosa*.
47
48
49
50

643 53 54 55 644 **4 Conclusions**

56
57
58
645 The presence of pharmaceuticals in marine macrophytes has been reported, but their effects on
59
60
646 seagrasses have not been assessed so far. This information may help in developing more effective
61
62
63
64
65

647 seagrass conservation strategies and management interventions. Our study demonstrates that a
1
648 short-term exposure of the seagrass *C. nodosa* to IBU concentrations detected in coastal seawaters
3
649 cannot elicit detrimental growth effects. However, it shows that this chemical causes oxidative
4
650 stress and damages the photosynthetic machinery, especially at the highest concentration. The
6
651 observed increased production of specific secondary metabolites and antioxidant compounds,
8
652 including acid gallic acid and rutin, as well as the enhancement of the excitation energy dissipation
10
653 of PSII and the acceleration of electron transport in the intersystem, could be an attempt of plants to
11
654 mitigate the effects of this pollutant. But the potential risks posed by a prolonged exposure to IBU
13
655 for seagrasses need to be assessed. Further studies should also monitor the behavior of IBU in
14
656 seagrass meadows and evaluate whether it makes them less resilient to other global environmental
15
657 stressors including climate changes.
16
17
18
19
20
21
22
23
24
25
26
27
28

659 **CRedit authorship contribution statement**

660 **Virginia Menicagli:** Methodology, Formal analysis, Investigation (plant harvesting, plant
31
661 cultivation, morphological trait and growth measurements), Visualization, Writing - Review &
32
662 Editing. **Monica Ruffini Castiglione:** Methodology, Formal analysis, Investigation (plants
33
663 histochemical assay), Visualization, Writing- Review & Editing, Funding acquisition. **Emily Cioni:**
34
664 Methodology, Formal analysis, Investigation (detection of IBU in plants and NSW, specialized
35
665 plant secondary metabolites), Visualization, Writing- Review & Editing. **Carmelina Spanò:**
36
666 Methodology, Formal analysis, Investigation (oxidative stress evaluation, photosynthetic pigments
37
667 measurement, antioxidant enzyme activity), Visualization, Writing - Review & Editing, Funding
38
668 acquisition. **Elena Balestri:** Conceptualization, Methodology, Formal analysis, Investigation (plant
39
669 harvesting, plant cultivation, morphological trait and growth measurements), Visualization,
40
670 Supervision, Writing - Review & Editing, Funding acquisition. **Marinella De Leo:** Methodology,
41
671 Formal analysis, Investigation (detection of IBU in plants and NSW, specialized plant secondary
42
672 metabolites), Visualization, Writing- Review & Editing, Funding acquisition. **Stefania Bottega:**
43
44
45
46
47
48
49
50
51
52
53
54
55
56
57
58
59
60
61
62
63
64
65

673 Methodology, Formal analysis, Investigation (oxidative stress evaluation, photosynthetic pigments
1
674 measurement, antioxidant enzyme activity), Visualization, Writing - Review & Editing. **Carlo**
3
675 **Sorce**: Methodology, Formal analysis, Investigation (photosynthetic efficiency measurements),
4
676 Visualization, Writing - Review & Editing, Funding acquisition. **Claudio Lardicci**:
6
677 Conceptualization, Methodology, Formal analysis, Investigation (plant harvesting, plant cultivation,
9
678 morphological trait and growth measurements), Writing – Review & Editing, Supervision, Funding
10
679 acquisition.
11
12
13
14
15

680

18

681

19

682

20

21

683

22

23

684

24

25

685

26

686

27

28

687

29

688

30

689

31

690

32

691

33

692

34

693

35

694

36

695

37

696

38

697

39

698

40

41

42

43

44

45

46

47

48

49

50

51

52

53

54

55

56

57

58

59

60

61

62

63

64

65

Declaration of competing interest

The authors declare that they have no known competing financial interests or personal relationships that could have influenced the work reported in this paper.

Acknowledgements and funding

We thank Giada Bernardini for her help in the experiment. This work was funded by Fondi di Ateneo (FA) of University of Pisa (Italy), and by the Italian Ministry of Universities and Research under the Department of Excellence 2023–2027 initiative.

References

- Adeleye, A.S., Xue, J., Zhao, Y., Taylor, A.A., Zenobio, J.E., Sun, Y., Han, Z., Salawu, O.A., Zhu, Y., 2022. Abundance, fate, and effects of pharmaceuticals and personal care products in aquatic environments. *J. Hazard. Mat.*, 424, 127284. <https://doi.org/10.1016/j.jhazmat.2021.127284>
- Aebi, H., 1984. Catalase in vitro. *Methods Enzymol.*, 105, 121-126. [https://doi.org/10.1016/S00766879\(84\)05016-3](https://doi.org/10.1016/S00766879(84)05016-3)
- Agostini, S., Pergent, M., Marchard, B., 2003. Growth and primary production of *Cymodocea nodosa* in a coastal lagoon. *Aquat. Bot.*, 185-193. [https://doi.org/10.1016/S0304-3770\(03\)00049-4](https://doi.org/10.1016/S0304-3770(03)00049-4)

- 699 Alfonso-Muniozguren, P., Serna-Galvis, E.A., Bussemaker, M., Torres-Palma, R.A., Lee, J., 2021.
1
700 A review on pharmaceuticals removal from waters by single and combined biological,
3
4
701 membrane filtration and ultrasound systems. *Ultrason. Sonochem.*, 76, 105656.
6
702 <https://doi.org/10.1016/j.ultsonch.2021.105656>
8
- 703 Ali, A.M., Thorsen Rønning, H., Sydnes, L.K., Alarif, W.M., Kallenborn, R., Al-Lihaibi, S.S., 2018.
10
704 Detection of PPCPs in marine organisms from contaminated coastal waters of the Saudi Red Sea.
11
12
705 *Sci. Total Environ.*, 621, 654-662. <https://doi.org/10.1016/j.scitotenv.2017.11.298>
14
15
- 706 Almeida, A., Sole, M., Soares, A.M.V.M., Freitas, R., 2020. Anti-inflammatory drugs in the marine
16
17
707 environment: Bioconcentration, metabolism and sub-lethal effects in marine bivalves. *Environ.*
18
19
708 *Pollut.*, 263, 114442. <https://doi.org/10.1016/j.envpol.2020.114442>
21
22
- 709 Álvarez-Muñoz, D., Rodríguez-Mozaz, S., Maulvault, A.L., Tediosi, A., Fernández-Tejedor, M.,
23
24
710 Van den Heuvel, F., Kotterman, M., Marques, A., Barceló, D., 2015. Occurrence of
25
26
711 pharmaceuticals and endocrine disrupting compounds in macroalgae, bivalves, and fish from
27
28
712 coastal areas in Europe. *Environ. Res.*, 143, 56-64.
29
30
713 <http://dx.doi.org/10.1016/j.envres.2015.09.018>
31
32
33
- 714 Ankley, G.T., Brooks, B.W., Huggett, D.B., Sumpter, J.P., 2007. Repeating history:
34
35
715 pharmaceuticals in the environment. *Environ. Sci. Technol.*, 41, 8211-8217.
36
37
716 <https://doi.org/10.1021/es072658j>
38
39
- 717 Arezki, O., Boxus, P., Kevers, C., Gaspar, T., 2001. Changes in peroxidase activity, and level of
40
41
718 phenolic compounds during light-induced plantlet regeneration from *Eucalyptus camaldulensis*
42
43
719 Dehn. nodes in vitro. *Plant Growth Regulation* 33, 215–219.
44
45
720 <https://doi.org/10.1023/A:1017579623170>
46
47
48
49
- 721 Astudillo-Pascual, M., Domínguez, I., Aguilera, P.A., Garrido Frenich, A., 2021. New phenolic
50
51
722 compounds in *Posidonia oceanica* seagrass: A comprehensive array using high resolution mass
52
53
54
55
723 spectrometry. *Plants*, 10, 864. <https://doi.org/10.3390/plants10050864>
56
57
58
59
60
61
62
63
64
65

- 724 Barbier, E.B., Hacker, S.D., Kennedy, C., Koch, E.W., Stier, A.C., Silliman, B., 2011. The value of
1
725 estuarine and coastal ecosystem services. *Ecol. Monogr.*, 81, 169–193.
3
4
726 <https://doi.org/10.1890/10-1510.1>
6
- 727 Bascuñán-Godoy L., Sanhueza C., Cuba M., Zuñiga G.E., Corcuera L.J., Bravo L.A., 2012. Cold-
8
728 acclimation limits low temperature induced photoinhibition by promoting a higher
10
11
729 photochemical quantum yield and a more effective PSII restoration in darkness in the Antarctic
13
14
730 rather than the Andean ecotype of *Colobanthus quitensis* Kunt Bartl (Cariophyllaceae). *BMC*
15
731 *Plant Biology*, 12, 114. <https://doi.org/10.1186/1471-2229-12-114>
18
- 732 Beyer, W.F., Fridovich, I., 1987. Assaying for superoxide dismutase activity: some large
20
733 consequences of minor changes in conditions. *Anal. Biochem.*, 161, 559-66.
21
22
734 [https://doi.org/10.1016/0003-2697\(87\)90489-1](https://doi.org/10.1016/0003-2697(87)90489-1)
25
- 735 Blasco, J., Trombini, C., 2023. Ibuprofen and diclofenac in the marine environment - a critical
26
27
736 review of their occurrence and potential risk for invertebrate species. *Water Emerg. Contam.*
30
737 *Nanoplastics.*, 2, 14. <https://dx.doi.org/10.20517/wecn.2023.06>
31
32
- 738 Borum, J., Duarte, C.M., Krause-Jensen, D., Greve, T.M., 2004. European seagrasses: an
33
34
739 introduction to monitoring and management. *Monitoring and managing of European seagrasses*
37
740 *Project (M&MS)*. 88.
40
- 741 Boudouresque, C.F., Bernard, G., Pergent, G., Shili, A., Verlaque, M., 2009. Regression of
42
742 Mediterranean seagrasses caused by natural processes and anthropogenic disturbances and stress:
43
44
743 a critical review. *Bot. Mar.*, 395–418. <https://doi.org/10.1515/BOT.2009.057>
45
47
- 744 Bradford, M.M., 1976. A rapid and sensitive method for the quantitation of microgram quantities of
48
49
745 protein utilizing the principle of protein-dye binding. *Anal. Biochem.*, 7, 248-54.
50
51
746 <https://doi.org/10.1006/abio.1976.9999>
54
- 747 Brain, R.A., Johnson, D.J., Richards, S.M., Sanderson, H., Sibley, P.K., Solomon, K.R., 2004.
55
56
748 Effects of 25 pharmaceutical compounds to *Lemna gibba* using a seven-day static-renewal test.
59
60
749 *Environ. Toxicol.*, 23, 371–382. <https://doi.org/10.1897/02-576>
61
62
63
64
65

- 750 Branchet, P., Arpin-Pont, L., Pirama, A., Boissery, P., Wong-Wah-Chung, P., Doumenq, P., 2021.
1
751 Pharmaceuticals in the marine environment: What are the present challenges in their monitoring?
3
752 Sci. Total Environ., 766, 142644. <https://doi.org/10.1016/j.scitotenv.2020.142644>
4
6
753 Cancemi, G., Buia, M.C., Mazzella, L., 2002. Structure and growth dynamics of *Cymodocea*
8
754 *nodosa* meadows. Scientia Marina, 66, 365-373.
9
10
11
755 Carazzone, C., Mascherpa, D., Gazzani, G., Papetti, A., 2013. Identification of phenolic
13
756 constituents in red chicory salads (*Cichorium intybus*) by high-performance liquid
14
15
16
757 chromatography with diode array detection and electrospray ionisation tandem mass
18
758 spectrometry. Food Chem., 138, 1062-1071. <https://doi.org/10.1016/j.foodchem.2012.11.060>
19
20
21
759 Cheng, H., Wang, X., Wang, J., Li, Q., 2021. Key photoprotective pathways of a shade-tolerant
22
23
760 plant (*Alpinia oxyphylla*) for precipitation patterns change during the dry season: thermal energy
25
761 dissipation and water-water cycle. Plant Stress 2, 100016.
26
27
28
762 <https://doi.org/10.1016/j.stress.2021.100016>
29
30
31
763 Cioni, E., De Leo, M., Cacciola, A., D'Angelo, V., Germanò, M.P., Camangi, F., Ricci, D., Fabene,
32
33
764 E., Diretto, G., De Tommasi, N., Braca, A., 2024. Re-discovering *Prunus* fruit varieties as
35
765 antiangiogenic agents by metabolomic and bioinformatic approach. Food Chem., 435, 137574.
36
37
38
766 <https://doi.org/10.1016/j.foodchem.2023.137574>
39
40
767 Daudi, A., O'Brien, J.A., 2012. Detection of Hydrogen Peroxide by DAB Staining in Arabidopsis
42
768 Leaves. Bio Protoc., 2:e263.
43
44
45
769 De Orte, M.R., Carballeira, C., Viana, I.G., Carballeira, A., 2013. Assessing the toxicity of chemical
47
770 compounds associated with marine land-based fish farms: The use of miniscale microalgal
48
49
50
771 toxicity tests. Chem. Ecol., <https://doi.org/10.1080/02757540.2013.790381>
52
53
772 Di Baccio, D., Pietrini, F., Bertolotto, P., Pérez, S., Barcelò, D., Zacchini, M., Donati, E., 2017.
54
55
773 Response of *Lemna gibba* L. to high and environmentally relevant concentrations of ibuprofen:
57
774 Removal, metabolism and morpho-physiological traits for biomonitoring of emerging
58
59
60
61
62
63
64
65

- 775 contaminants. *Sci. Total Environ.*, 584-585, 363–373.
1
776 <http://dx.doi.org/10.1016/j.scitotenv.2016.12.191>
3
4
777 Ding, T., Yang, M., Zhang, J., Yang, B., Lin, K., Li, J., Gan, J., 2017. Toxicity, degradation and
6
778 metabolic fate of ibuprofen on freshwater diatom *Navicula* sp. *J. Hazard. Mat.*, 330, 127-134.
8
779 <http://dx.doi.org/10.1016/j.jhazmat.2017.02.004>
10
11
780 EU, 2013. Directive 2013/39/EU of the European Parliament and of the Council of 12 August 2013
13
781 amending Directives 2000/60/EC and 2008/105/EC as regards priority substances in the field of
14
15
16
782 water policy.
18
783 Fernández-Fernández, R., López-Martínez, J.C., Romero-González, R., Martínez-Vidal, J.L.,
20
784 Alarcón Flores, M.I., Garrido Frenich, A., 2010. Simple LC–MS determination of citric and
21
22
23
785 malic acids in fruits and vegetables. *Chromatographia*, 72, 55-62.
25
786 <https://doi.org/10.1365/s10337-010-1611-0>
26
27
28
787 Ferreira, B.L., Ferreira, D.P., Borges, S.F., Ferreira, A.M., Holanda, F.H., Ucella-Filho, J.G.M.,
30
788 Cruz, R.A.S., Birolli, W.G., Luque, R., Ferreira, I.M., 2023. Diclofenac, ibuprofen, and
31
32
33
789 paracetamol biodegradation: overconsumed non-steroidal anti-inflammatory drugs at COVID-
35
36
790 19 pandemic. *Front. Microbiol.*, 14, 1207664. <https://doi.org/10.3389/fmicb.2023.1207664>
37
38
791 García-Marquez, M.G., Rodríguez-Castañeda, J.C., Agawin, N.S.R., 2023. Sunscreen exposure
40
792 interferes with physiological processes while inducing oxidative stress in seagrass *Posidonia*
42
793 *oceanica* (L.) Delile. *Mar. Pollut. Bull.*, 187, 114507.
43
44
45
794 <https://doi.org/10.1016/j.marpolbul.2022.114507>
47
48
795 Giorgetti, L., Spanò, C., Muccifora, S., Bellani, L., Tassi, E., Bottega, S., Di Gregorio, S., Siracusa,
49
50
796 G., Sanità di Toppi, L., Ruffini Castiglione, M., 2019. An integrated approach to highlight
52
797 biological responses of *Pisum sativum* root to nano-TiO₂ exposure in a biosolid-amended
53
54
55
798 agricultural soil. *Sci. Tot. Environ.* 650, 2705-2716.
57
799 <https://doi.org/10.1016/j.scitotenv.2018.10.032>
59
60
61
62
63
64
65

- 800 Gonzales-Rey, M., Bebianno, M.J., 2011. Non-steroidal anti-inflammatory drug (NSAID) ibuprofen
1
801 distresses antioxidant defense system in mussel *Mytilus galloprovincialis* gills. *Aquat. Toxicol.*,
2
3
4
802 105, 264-269. <https://doi.org/10.1016/j.aquatox.2011.06.015>
5
6
- 803 Gorni, P.H., de Lima, G.R., de Oliveira Pereira, L.M., Spera, K.D., de Marcos Lapaz, A., Pacheco,
7
8
9
804 A.C., 2022. Increasing plant performance, fruit production and nutritional value of tomato
10
11
805 through foliar applied rutin. *Sci. Hortic.*, 294, 110755.
12
13
806 <https://doi.org/10.1016/j.scienta.2021.110755>
14
15
- 807 Grignon-Dubois, M., Rezzonico, B., 2013. The economic potential of beach-cast seagrass—
16
17
18
808 *Cymodocea nodosa*: a promising renewable source of chicoric acid. *Bot. Mar.*, 56, 303-311.
19
20
809 <https://doi.org/10.1515/bot-2013-0029>
21
22
23
- 810 Gupta, R., 2020. The oxygen-evolving complex: a super catalyst for life on earth, in response to
24
25
811 abiotic stresses. *Plant Signaling and Behavior*, 15, 12.
26
27
812 <https://dx.doi.org/10.1080/15592324.2020.1824721>
28
29
30
- 813 Hassanzadeh, M., Ebadi, A., Panahyan-e-Kivi, M., Eshghi, A.G., Sh, Jamaati-e-Somarin, Saeidi,
31
32
33
814 M., Zabihi-e-Mahmoodabad, R., 2009. Evaluation of drought stress on relative water content and
34
35
815 chlorophyll content of Sesame (*Sesamum indicum* L.) genotypes at early flowering stage. *Res. J.*
36
37
816 *Environ. Sci.* 3,345-360.
38
39
40
- 817 He, Y., Langenhoff, A.A.M., Sutton, N.B., Rijnaarts, H.H.M., Blokland, M.H., Chen, F., Huber, C.,
41
42
43
818 Schröder, P., 2017. Metabolism of Ibuprofen by *Phragmites australis*: Uptake and
44
45
819 phytodegradation. *Environ. Sci. Technol.*, 51, 4576–4584.
46
47
820 <https://doi.org/10.1021/acs.est.7b00458>
48
49
50
- 821 Ibanez, M., Bijlsma, L., Pitarch, E., López, F.J., Hernández, F., 2021. Occurrence of pharmaceutical
51
52
53
822 metabolites and transformation products in the aquatic environment of the Mediterranean area.
54
55
823 *Trends Environ. Anal. Chem.*, 29, e00118. <http://dx.doi.org/10.1016/j.teac.2021.e00118>
56
57
58
59
60
61
62
63
64
65

- 824 Iori, V., Zacchini, M., Pietrini, F., 2013. Growth, physiological response and phytoremoval
1
825 capability of two willow clones exposed to ibuprofen under hydroponic culture. J. Hazard. Mat.,
2
3
4
826 262, 796–804. <https://dx.doi.org/10.1016/j.jhazmat.2013.09.017>
5
6
- 827 Ismail, H., Maksimović, J.D., Maksimović, V., Shabala, L., Živanović, B.D., Tian, Y., Jacobsen,
7
8
9
828 S.E., Shabala, S., 2015. Rutin, a flavonoid with antioxidant activity, improves plant salinity
10
11
829 tolerance by regulating K⁺ retention and Na⁺ exclusion from leaf mesophyll in quinoa and broad
12
13
830 beans. Func. Plant Bio., 43, 75-86. <https://doi.org/10.1071/FP15312>
14
15
16
- 831 Jana, S., Choudhuri, M.A., 1982. Glycolate metabolism of three submersed aquatic angiosperms
17
18
832 during ageing. Aquatic Bot. 12, 345-354. [https://doi.org/10.1016/0304-3770\(82\)90026-2](https://doi.org/10.1016/0304-3770(82)90026-2)
19
20
21
- 833 Kock, A., Glanville, H.C., Law, A.C., Stanton, T., Carter, L.J., Taylor, J.C., 2023. Emerging
22
23
834 challenges of the impacts of pharmaceuticals on aquatic ecosystems: A diatom perspective. Sci.
24
25
835 Total Environ., 878, 162939. <http://dx.doi.org/10.1016/j.scitotenv.2023.162939>
26
27
28
- 836 Krüger, G.H.J., De Villiers, M.F., Strauss, A.J., de Beer, M., van Heerden, P.D.R., Maldonado, R.,
29
30
837 Strasser, R.J., 2014. Inhibition of photosystem II activities in soybean (*Glycine max*) genotypes
31
32
838 differing in chilling sensitivity. S. Afr. J. Bot., 95, 85–96.
33
34
839 <https://doi.org/10.1016/j.sajb.2014.07.010>
35
36
37
38
- 840 Kuo, J., den Hartog, C., 2006. Seagrass morphology, anatomy, and ultrastructure, in: Larkum,
39
40
841 A.W.D., Orth, R.J., Duarte, C.M. (Ed.), 2006. Seagrasses: biology, ecology and conservation.
41
42
842 Springer: Dordrecht. <https://dx.doi.org/10.1007/978-1-4020-2983-7>
43
44
45
- 843 Lewis, M.A., Devereux, R., 2009. Non nutrient anthropogenic chemicals in seagrass ecosystems:
46
47
844 fate and effects. Environ. Toxicol. Chem., 3, 644–661. <https://doi.org/10.1897/08-201.1>
48
49
50
- 845 Li, Y., Zhang, J., Zhu, G., Liu, Y., Wu, B., Ng, W.J., Appan, A., Tanet, S.K., 2016.
51
52
846 Phytoextraction, phytotransformation and rhizodegradation of ibuprofen associated with *Typha*
53
54
847 *angustifolia* in a horizontal subsurface flow constructed wetland. Water Res., 102, 294-304.
55
56
848 <http://dx.doi.org/10.1016/j.watres.2016.06.049>
57
58
59
60
61
62
63
64
65

- 849 Li, Y., Chen, F., Zhou, R., Zheng, X., Pan, K., Qiu, G., Wu, Z., Chen, S., Wang, D., 2023. A review
1
850 of metal contamination in seagrasses with an emphasis on metal kinetics and detoxification. J.
2
3
4
851 Hazard Mat., 454, 131500. <https://doi.org/10.1016/j.jhazmat.2023.131500>
5
6
- 852 Lichtenthaler, H.K., 1987. Chlorophylls and carotenoids: Pigments of photosynthetic
7
8
9
853 biomembranes. *Methods Enzymol.*, 148, 350-382. [https://doi.org/10.1016/0076-6879\(87\)480361](https://doi.org/10.1016/0076-6879(87)480361)
10
11
- 854 Lijia, X., Guo, J., Chen, Q., Baoping, J., Zhang, W., 2014. Quantitation of phlorizin and phloretin
12
13
14
855 using an ultra high-performance liquid chromatography–electrospray ionization tandem mass
15
16
856 spectrometric method. *J. Chromatogr. B*, 960, 67-72.
17
18
857 <https://doi.org/10.1016/j.jchromb.2014.04.007>
19
20
- 858 Long, B.M., Harriage, S., Schultz, N.L., Sherman, C.D.H., B., Thomas, M., 2023. Pharmaceutical
21
22
23
859 pollution in marine waters and benthic flora of the southern Australian coastline. *Environ.*
24
25
860 *Chem.*, 19, 375–384. <https://doi.org/10.1071/EN22054>
26
27
28
- 861 Loos, R., Tavazzi, S., Paracchini, B., Canuti, E., Weissteiner, C., 2013. Analysis of polar organic
29
30
31
862 contaminants in surface water of the northern Adriatic Sea by solid-phase extraction followed by
32
33
863 ultrahigh-pressure liquid chromatography–QTRAP® MS using a hybrid triple-quadrupole linear
34
35
864 ion trap instrument. *Anal. Bioanal. Chem.*, 405, 5875–5885. [https://doi.org/10.1007/s00216-013-
36
37
38
865 6944-8](https://doi.org/10.1007/s00216-013-6944-8)
39
40
- 866 López-Fernández, O., Domínguez, R., Pateiro, M., Munekata, P.E., Rocchetti, G., Lorenzo, J.M.,
41
42
43
867 2020. Determination of polyphenols using liquid chromatography–tandem mass spectrometry
44
45
868 technique (LC–MS/MS): a review. *Antioxidants*, 9, 479. <https://doi.org/10.3390/antiox9060479>
46
47
48
- 869 Madikizela, L.M., Ncube, S., Tutu, H., Richards, H., Newman, B., Ndungu, K., Chimuka, L., 2020.
49
50
870 Pharmaceuticals and their metabolites in the marine environment: Sources, analytical methods
51
52
53
871 and occurrence. *Trends Environ. Anal. Chem.*, 28, e00104.
54
55
872 <http://dx.doi.org/10.1016/j.teac.2020.e00104>
56
57
58
59
60
61
62
63
64
65

- 873 Makino, A., Miyake, C., Yokota, A., 2002. Physiological functions of the water–water cycle
1
874 (Mehler Reaction) and the cyclic electron flow around PSI in rice leaves. *Plant Cell Physiol.*, 43,
2
3
4
875 1017–1026. <https://doi.org/10.1093/pcp/pcf124>
5
6
- 876 Malea, P., Kevrekidis, T., Chatzipanagiotou, K.-R., Mogias, A., 2018. Cadmium uptake kinetics in
7
8
9
877 parts of the seagrass *Cymodocea nodosa* at high exposure concentrations. *J. Biol. Res-*
10
11
878 *Thessaloniki*, 25, 5. <https://doi.org/10.1186/s40709-018-0076-4>
12
13
- 879 Maranhão, L.A., DelValls, T.A., Martín-Díaz, M.L., 2015. Assessing potential risks of wastewater
14
15
880 discharges to benthic biota: an integrated approach to biomarker responses in clams (*Ruditapes*
16
17
881 *philippinarum*) exposed under controlled conditions. *Mar. Pollut. Bull.* 92, 11–24.
18
19
20
882 <https://doi.org/10.1016/j.marpolbul.2015.01.009>
21
22
23
- 883 Marbà, N., Krause-Jensen, D., Alcoverro, T., Birk, S., Pedersen, A., Neto, J.M., Orfanidis, S.,
24
25
884 Garmendia, J.M., Muxika, I., Borja, A., Dencheva, K., Duarte, C.M., 2013. Diversity of
26
27
885 European seagrass indicators: patterns within and across regions. *Hydrobiologia*, 1–14.
28
29
30
886 <https://doi.org/10.1007/s10750-012-1403-7>
31
32
33
- 887 Matozzo, V., Rova, S., Marin, M.G., 2012. The nonsteroidal anti-inflammatory drug, ibuprofen,
34
35
888 affects the immune parameters in the clam *Ruditapes philippinarum*. *Mar. Environ. Res.*, 79,
36
37
889 116–121. <http://dx.doi.org/10.1016/j.marenvres.2012.06.003>
38
39
40
- 890 McMahon, K., Kilminster, K., Canto, R., Roelfsema, C., Lyons, M., Kendrick, G.A., Waycott, M.,
41
42
891 Udy, J., 2022. The risk of multiple anthropogenic and climate change threats must be considered
43
44
892 for continental scale conservation and management of seagrass habitat. *Front. Mar. Sci.*, 9,
45
46
893 837259. <https://doi.org/10.3389/fmars.2022.837259>
47
48
49
50
- 894 Menicagli, V., Balestri, E., Vallerini, F., De Battisti, D., Lardicci, C., 2021. Plastics and
51
52
895 sedimentation foster the spread of a non-native macroalga in seagrass meadows. *Sci. Total*
53
54
896 *Environ.*, 757, 143812. <https://doi.org/10.1016/j.scitotenv.2020.143812>
55
56
57
- 897 Menicagli, V., Ruffini Castiglione, M., Balestri, E., Giorgetti, L., Bottega, S., Sorce, C., Spanò, C.,
58
59
898 Lardicci, C., 2022. Early evidence of the impacts of microplastic and nanoplastic pollution on
60
61
62
63
64
65

- 899 the growth and physiology of the seagrass *Cymodocea nodosa*. *Sci. Total Environ.*, 838, 156514.
900 <http://dx.doi.org/10.1016/j.scitotenv.2022.156514>
- 901 Mezzelani, M., Regoli, F., 2022. The biological effects of pharmaceuticals in the marine
902 environment. *Ann. Rev. Mar. Sci.*, 14, 105–28. <https://doi.org/10.1146/annurev-marine-040821075606>
- 903
904 Mezzelani, M., Gorbi, S., Fattorini, D., d’Errico, G., Consolandi, G., Milan, M., Bargelloni, L.,
905 Regoli, F., 2018. Long-term exposure of *Mytilus galloprovincialis* to diclofenac, Ibuprofen and
906 Ketoprofen: Insights into bioavailability, biomarkers and transcriptomic changes. *Chemosphere*,
907 198, 238-248. <https://doi.org/10.1016/j.chemosphere.2018.01.148>
- 908 Milović, S., Stanković, I., Nikolić, D., Radović, J., Kolundžić, M., Nikolić, V., Stanojković, T.,
909 Petović, S., Kundaković-Vasović, T., 2019. Chemical analysis of selected seaweeds and seagrass
910 from the Adriatic Coast of Montenegro. *Chem. Biodiversity*, 16, e1900327.
911 <https://doi.org/10.1002/cbdv.201900327>
- 912 Montefalcone, M., 2009. Ecosystem health assessment using the Mediterranean sea-grass *Posidonia*
913 *oceanica*: a review. *Ecol. Indic.* 9, 595–604. <https://doi.org/10.1016/j.ecolind.2008.09.013>
- 914 Nakano, Y., Asada, K., 1981. Hydrogen peroxide is scavenged by ascorbate-specific peroxidase in
915 spinach chloroplasts. *Plant Cell Physiol.*, 22, 867–880.
916 <https://doi.org/10.1093/oxfordjournals.pcp.a076232>
- 917 Navarro, M., Moreira, I., Arnaez, E., Quesada, S., Azofeifa, G., Vargas, F., Alvarado, D., Chen, P.,
918 2018. Polyphenolic characterization and antioxidant activity of *Malus domestica* and *Prunus*
919 *domestica* cultivars from Costa Rica. *Foods*, 7, 15. <https://doi.org/10.3390/foods7020015>
- 920 Navarro-Hoyos, M., Arnáez-Serrano, E., Quesada-Mora, S., Azofeifa-Cordero, G., Wilhelm-
921 Romero, K., Quirós-Fallas, M.I., Alvarado-Corella, D., Vargas-Huertas, F., Sánchez-Kopper,
922 A., 2021. Polyphenolic QTOF-ESI MS characterization and the antioxidant and cytotoxic
923 activities of *Prunus domestica* commercial cultivars from Costa Rica. *Molecules*, 26, 6493.
924 <https://doi.org/10.3390/molecules26216493>

- 925 Oskarsson, H., Eriksson Wiklund, A.-K., Lindh, K., Kumblad, L., 2012. Effect studies of human
1
926 pharmaceuticals on *Fucus vesiculosus* and *Gammarus* spp. Mar. Environ. Res., 74, 1-8.
3
927 <https://doi.org/10.1016/j.marenvres.2011.11.001>
4
6
- 928 Ostrowski, W., Wojakowska, A., Grajzer, M., Stobiecki, M., 2014. Mass spectrometric behavior of
8
929 phenolic acids standards and their analysis in the plant samples with LC/ESI/MS system. J.
9
10
930 Chromatogr. B, 967, 21-27. <https://doi.org/10.1016/j.jchromb.2014.07.005>
11
13
- 931 Paunov, M., Koleva, L., Vassilev, A., Vangronsveld, J., Goltsev, V., 2018. Effects of different
14
15
932 metals on photosynthesis: Cadmium and Zinc affect chlorophyll fluorescence in durum wheat.
16
18
933 Int. J. Mol. Sci., 19, 787. <https://doi.org/10.3390/ijms19030787>
19
20
- 934 Pfeifer, L., Classen, B., 2020. The cell wall of seagrasses: Fascinating, peculiar and a blank canvas
21
22
935 for future research. Front. Plant Sci., 11, 588754. <https://doi.org/10.3389/fpls.2020.588754>
23
25
- 936 Pietrini, F., Di Baccio, D., Aceña, J., Pérez, S., Barceló, D., Zacchini, M., 2015. Ibuprofen exposure
26
27
937 in *Lemna gibba* L.: Evaluation of growth and phytotoxic indicators, detection of ibuprofen and
28
30
938 identification of its metabolites in plant and in the medium. J. Hazard Mat., 300, 189-193.
31
32
939 <http://dx.doi.org/10.1016/j.jhazmat.2015.06.068>
33
35
- 940 Pomati, F., Netting, A.G., Calamari, D., Neilan, B.A., 2004. Effects of erythromycin, tetracycline
36
37
941 and ibuprofen on the growth of *Synechocystis* sp. and *Lemna minor*. Aquat. Toxicol., 67, 387-
38
40
942 396. <https://doi.org/10.1016/j.aquatox.2004.02.001>
41
42
- 943 Rainsford, K.D., 2009. Ibuprofen: pharmacology, efficacy and safety. Inflammopharmacology, 17,
43
44
944 275-342.
45
47
- 945 R Core Team, 2018. R: A Language and Environment for Statistical Computing. R Foundation for
48
49
946 Statistical Computing, Vienna. <https://www.R-project.org>
50
52
- 947 Sánchez-Rabaneda, F., Jáuregui, O., Casals, I., Andrés-Lacueva, C., Izquierdo-Pulido, M.,
53
54
948 Lamuela-Raventós, R.M., 2003. Liquid chromatographic/electrospray ionization tandem mass
55
57
949 spectrometric study of the phenolic composition of cocoa (*Theobroma cacao*). J. Mass
58
59
950 Spectrom., 38, 35-42. <https://doi.org/10.1002/jms.395>
60
61
62
63
64
65

- 951 Sandrini-Neto, L., Camargo, M.G., 2014. GAD: An R Package for ANOVA Designs From General
1
2 Principles. R Package.
- 952
3
4
953 Silva, M., Feijão, E., da Cruz de Carvalho, R., Duarte, I.A., Matos, A.R., Cabrita, M.T., Barreiro,
5
6
954 A., Lemos, M.F.L., Novais, S.C., Marques, J.C., Caçador, I., Reis-Santos, P., Fonseca, V.F.,
7
8
955 Duarte, B., 2020. Comfortably numb: Ecotoxicity of the non-steroidal anti-inflammatory drug
9
10
956 ibuprofen on *Phaeodactylum tricornutum*. Mar. Environ. Res., 161, 105109.
11
12
957 <https://doi.org/10.1016/j.marenvres.2020.105109>
13
14
958 Spanò, C., Bruno, M., Bottega, S., 2013. *Calystegia soldanella*: dune versus laboratory plants to
15
16
959 highlight key adaptive physiological traits. Acta Physiol. Plant 35, 1329-1336.
17
18
960 <https://doi.org/10.1007/s11738-012-1173-x>
19
20
961 Spanò, C., Bottega, S., 2016. Durum wheat seedlings in saline conditions: salt spray versus root-
21
22
962 zone salinity. Estuar. Coast. Shelf Sci. 169, 173-181. <https://doi.org/10.1016/j.ecss.2015.11.031>
23
24
963 Spanò, C., Bottega, S., Ruffini Castiglione, M., Pedranzani, H.E., 2017. Antioxidant response to
25
26
964 cold stress in two oil plants of the genus *Jatropha*. Plant Soil Environ. 63, 271-276.
27
28
965 <https://doi.org/10.17221/182/2017-PSE>
29
30
966 Spanò, C., Bottega, S., Bellani, L., Muccifora, S., Sorce, C., Ruffini Castiglione, M., 2020. Effect of
31
32
967 zinc priming on salt response of wheat seedlings: relieving or worsening? Plants 9, 1514.
33
34
968 <https://doi.org/10.3390/plants9111514>
35
36
969 Stirbet, A., Lazár, D., Kromdijk, J., Govindjee, 2018. Chlorophyll a fluorescence induction: Can
37
38
970 just a one-second measurement be used to quantify abiotic stress responses? Photosynthetica, 56,
39
40
971 86-104. <https://doi.org/10.1007/s11099-018-0770-3>
41
42
972 Świacka, K., Maculewicz, J., Smolarz, K., Szaniawska, A., Caban, M., 2019. Mytilidae as model
43
44
973 organisms in the marine ecotoxicology of pharmaceuticals - a review. Environ. Pollut. 254,
45
46
974 113082. <https://doi.org/10.1016/j.envpol.2019.113082>
47
48
49
50
51
52
53
54
55
56
57
58
59
60
61
62
63
64
65

- 975 Świacka, K., Maculewicz, J., Kowalska, D., Caban, M., Smolarz, K., Świeszak, J., 2022. Presence of
1
976 pharmaceuticals and their metabolites in wild-living aquatic organisms – Current state of
3
977 knowledge. *J. Hazard. Mat.*, 424, 127350. <https://doi.org/10.1016/j.jhazmat.2021.127350>
4
6
978 Togola, A., Budzinski, H., 2008. Multi-residue analysis of pharmaceutical compounds in aqueous
8
979 samples. *J. Chromatogr. A.*, 1177, 150–158. <https://doi.org/10.1016/j.chroma.2007.10.105>
9
10
980 Tsimilli-Michael, M., 2020. Revisiting JIP-test: An educative review on concepts, assumptions,
13
981 approximations, definitions and terminology. *Photosynthetica*, 58, 275–292.
14
15
982 <https://doi.org/10.32615/ps.2019.150>
16
18
983 Vione, D., Reddy Maddigapu, P., De Laurentiis, E., Minella, M., Pazzi, M., Maurino, V., Minero,
20
984 C., Kouras, S., Richard, C., 2011. Modelling the photochemical fate of ibuprofen in surface
21
22
985 waters. *Water Res.*, 45, 6725-6736. <https://doi.org/10.1016/j.watres.2011.10.014>
23
24
25
986 Wang, C., Wang, Z., Wang, G., Yiu-Nam Lau, J., Zhang, K., Li, W., 2021. COVID-19 in early 2021:
26
27
987 current status and looking forward. *Signal. Transduct. Target. Ther.*, 6, 114.
28
29
30
988 <https://doi.org/10.1038/s41392-021-00527-1>
31
32
33
989 Wijaya, L., Alyemini, M., Ahmad, P., Alfarhan, A., Barcelo, D., El-Sheikh, M.A., Pico, Y., 2020.
34
35
990 Ecotoxicological effects of Ibuprofen on plant growth of *Vigna unguiculata* L. *Plants*, 9, 1473.
36
37
991 <https://doi.org/10.3390/plants9111473>
38
39
40
992 Wilton, C.C., Brant, R.B., 2013. *Ibuprofen: Clinical pharmacology, medical uses and adverse effects.*
41
42
993 Nova Science Press, New York.
43
44
45
994 Wiklund, A.-K. E., Oskarsson, H., Thorsén, G., Kumblad, L., 2011. Behavioural and physiological
46
47
995 responses to pharmaceutical exposure in macroalgae and grazers from a Baltic Sea littoral
48
49
50
996 community. *Aquat. Biol.*, 14, 29-39. <https://doi.org/10.3354/ab00380>
51
52
53
997 Yamamoto, Y., Kobayashi, Y., Matsumoto, H., 2001. Lipid peroxidation is an early symptom
54
55
998 triggered by aluminum, but not the primary cause of elongation inhibition in pea roots. *Plant*
56
57
999 *Physiol.*, 125, 199–208. <https://doi.org/10.1104/pp.125.1.199>
58
59
60
61
62
63
64
65

1000 Zagorchev, L., Atanasova, A., Albanova, I., Traianova, A., Mladenov, P., Kouzmanova, M.,
1
1001 Goltsev, V., Kalaji, H.M., Teofanova, D., 2021. Functional characterization of the
2
3
4
1002 photosynthetic machinery in smicronix galls on the parasitic plant *Cuscuta campestris* by JIP-
5
6
1003 Test. Cells, 10, 1399. <https://doi.org/10.3390/cells10061399>
7
8
9
1004 Zhang, X., Ran, W., Ye, M., Lin, S., Liu, M., Sun, X., 2022. Exogenous application of gallic acid
10
11
1005 induces the direct defense of tea plant against *Ectropis obliqua* Caterpillars. Front. Plant Sci., 13,
12
13
1006 833489. <https://doi.org/10.3389/fpls.2022.833489>
14
15
16
1007
17
18
1008
19
20
1009
21
22
23
24
1010
25
26
27
1011
28
29
30
1012
31
32
33
1013
34
35
36
1014
37
38
39
40
1015
41
42
1016
43
44
45
1017
46
47
1018
48
49
50
1019
51
52
1020
53
54
55
1021
56
57
1022
58
59
1023
60
61
62
63
64
65

1024 **Figure Legends**

1
1025 **Figure 1** *Cymodocea nodosa* plants exposed to different levels of seawater contamination by IBU
3
4
1026 (0 $\mu\text{g L}^{-1}$ or Control-Ctrl, 0.25 $\mu\text{g L}^{-1}$ or Low, 2.5 $\mu\text{g L}^{-1}$ or Medium, 25 $\mu\text{g L}^{-1}$ or High) at the
6
1027 beginning and at the end of the experiment.

9
1028 *2-columns fitting image, color in the online version only*

1029
1030 **Figure 2** Comparison of qualitative profiles of *Cymodocea nodosa* extracts from plants exposed to
13
14
15
1031 high (H) concentrations of IBU and control plants (C) grown without IBU. LC-MS/MS analyses were
17
1032 recorded in negative ion mode. Each number corresponds to those listed in Table S5.

19
20
1033 *2-columns fitting image, color in the online version only*

22
1034
24
1035 **Figure 3** Phenolic acids (a) and flavonoids (b) found in the extracts of plants treated with high (H)
25
26
1036 and medium (M) IBU concentrations differing significantly (* = $p < 0.05$; ** = $p < 0.005$) in
28
29
1037 amount ($\mu\text{g g}^{-1}$ FW) from the control group (C). GA = gallic acid; HBAd = hydroxybenzoic acid
30
31
1038 derivative; DHBAH = dihydroxybenzoic acid hexoside; HMBAd = hydroxymethylbenzoic acid
33
1039 derivative; DHCAd = dihydrocoumaric acid derivative; CH(I) and CH(II) = coumaroyl hexoside
35
36
1040 isomers; FH = feruloylhexoside; CA = coumaric acid; CMA = coumaroylmalic acid; FMA =
38
1041 feruloylmalic acid; R = rutin; KH = kaempferol hexoside; IH = isorhamnetin hexoside; NH =
40
41
1042 naringenin hexoside; IAH = isorhamnetin acetylhexoside; IMH = isorhamnetin malonylhexoside; I
43
1043 = isorhamnetin.

45
46
1044 *Single column fitting image, color in the online version only*

48
1045
50
51
1046 **Figure 4** Concentration of (a,b) hydrogen peroxide (H_2O_2) and (c,d) thiobarbituric acid reactive
52
53
1047 substances (TBARS) in rhizome (left column) and leaves (right column) of *Cymodocea nodosa*
55
56
1048 plants exposed to different levels of seawater contamination by IBU (0 $\mu\text{g L}^{-1}$ or control-Ctrl, 0.25
57
58
1049 $\mu\text{g L}^{-1}$ or Low, 2.5 $\mu\text{g L}^{-1}$ or Medium, 25 $\mu\text{g L}^{-1}$ or High). Different letters denote significant
60
1050 differences ($p < 0.05$) among treatments. Mean \pm SE, $n = 4$.

1051 *1.5-column fitting image, color in the online version only*

1
2
1052
3
4
1053
5
6
1054
7
8
1055
9
10
11
1056
12
13
1057
14
15
16
1058
17
18
1059
19
20
21
1060
22
23
1061
24
25
1062
26
27
28
1063
29
30
1064
31
32
33
1065
34
35
1066
36
37
1067
38
39
40
1068
41
42
1069
43
44
45
1070
46
47
1071
48
49
50
1072
51
52
1073
53
54
55
1074
56
57
1075
58
59
1076
60
61
62
63
64
65

Figure 5 Representative images of rhizome cross sections of *Cymodocea nodosa* plants processed to histochemical detection of oxidative stress markers. Amplex probe (H₂O₂ indicator, images left) and Bodipy probe (lipid peroxidation indicator, images right). a, b = control; c, d = low IBU concentration; e, f = medium IBU concentration; g, h = high IBU concentration. Scale bar = 100 μ m.

2-columns fitting image, color in the online version only

Figure 6 Representative images of leaf portions of *Cymodocea nodosa* plants processed to histochemical detection of H₂O₂ by DAB staining. Tip-leaf segments, images left; mid-leaf segments, images right. a, b = control; c, d = low IBU concentration; e, f = medium IBU concentration; g, h = high IBU concentration. Scale bar = 1 mm.

2-columns fitting image, color in the online version only

Figure 7. Representative images of leaf portions of *Cymodocea nodosa* plants processed to histochemical detection of lipid peroxidation by Schiff[®] reagent staining. Tip-leaf segments, images left; mid-leaf segments, images right. a, b = control; c, d = low IBU concentration; e, f = medium IBU concentration; g, h = high IBU concentration. Scale bar = 1 mm.

2-columns fitting image, color in the online version only

Figure 8 Effects of the exposure to 25 μ g L⁻¹ IBU for (a) 5 days and (b, c) 12 days in dark-adapted *Cymodocea nodosa* leaves. The bar plots report the parameters of JIP test (described in Table S2), normalized to the values of the control, which were set as one. Dashed lines = control (value = 1). Only those parameters that differed significantly from the control ($p < 0.05$) are shown. All values are the mean of five replicates.

Single column fitting image, color in the online version only

1077

1

1078

2

3

4

5

6

7

8

9

10

11

12

13

14

15

16

17

18

19

20

21

22

23

24

25

26

27

28

29

30

31

32

33

34

35

36

37

38

39

40

41

42

43

44

45

46

47

48

49

50

51

52

53

54

55

56

57

58

59

60

61

62

63

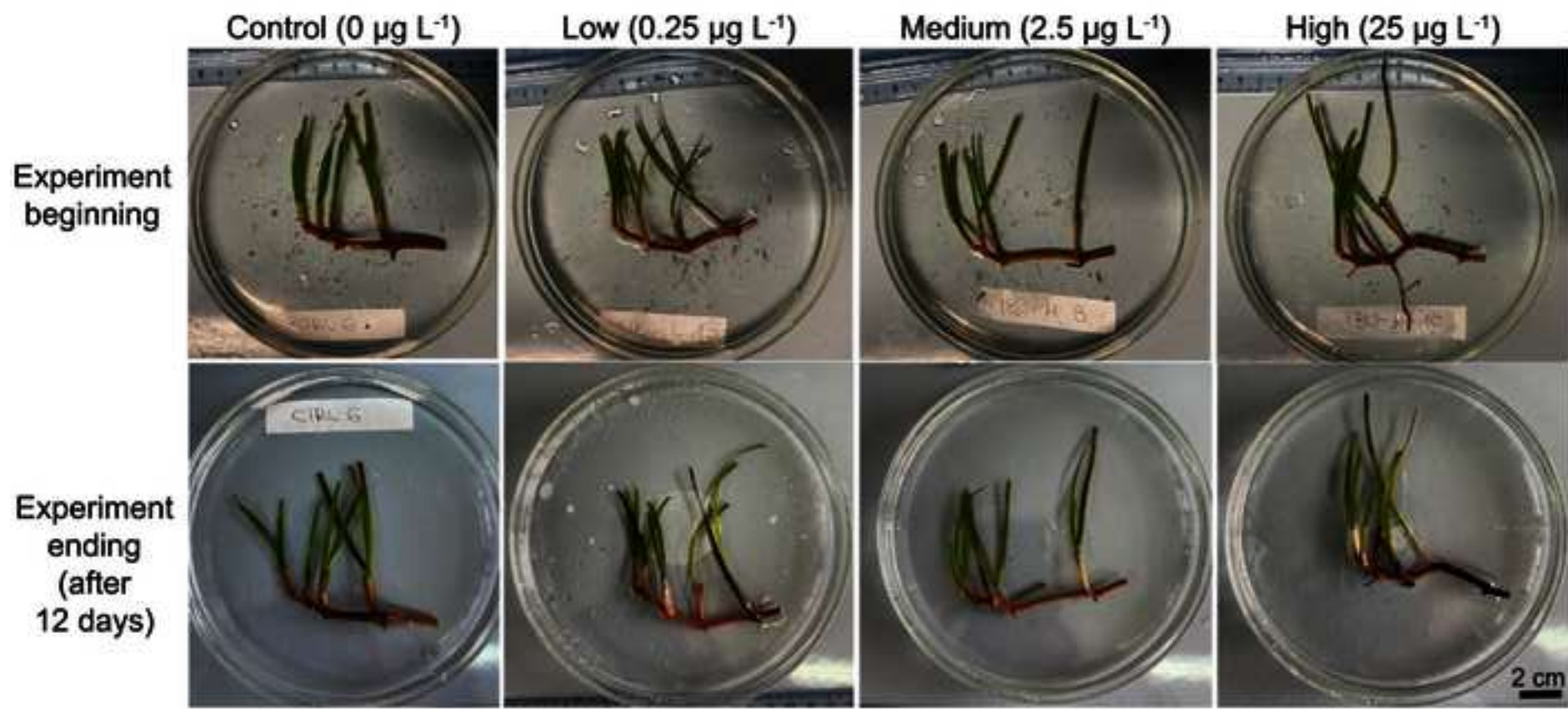
64

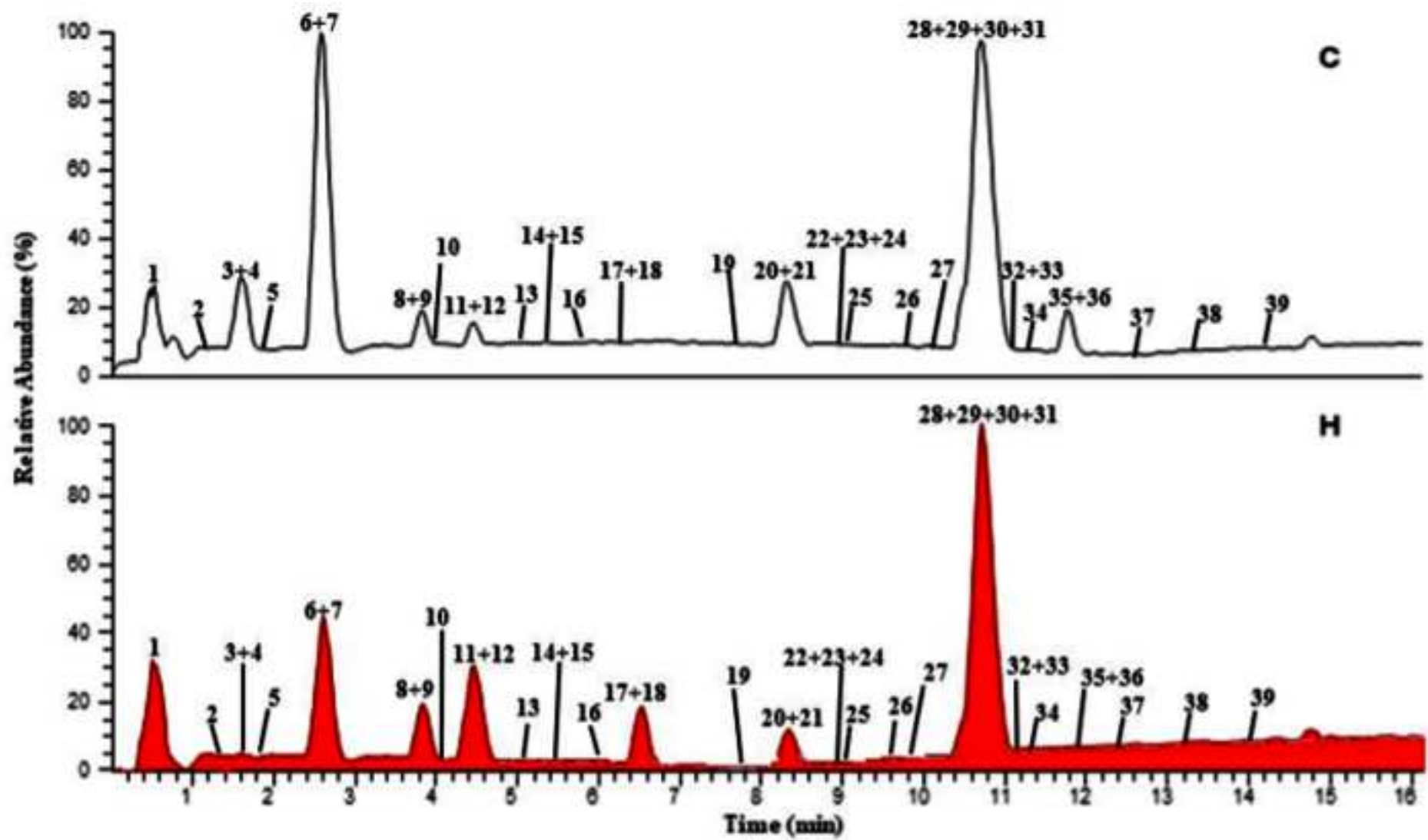
65

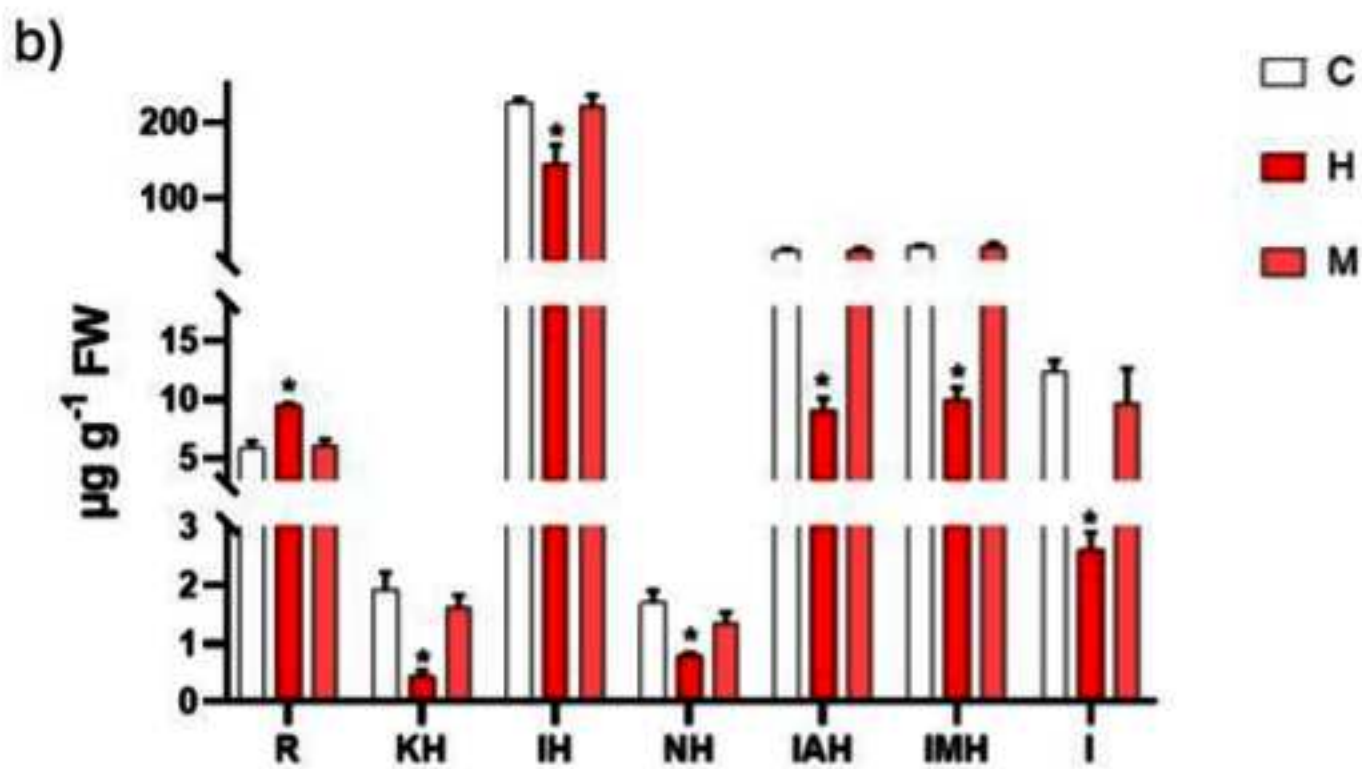
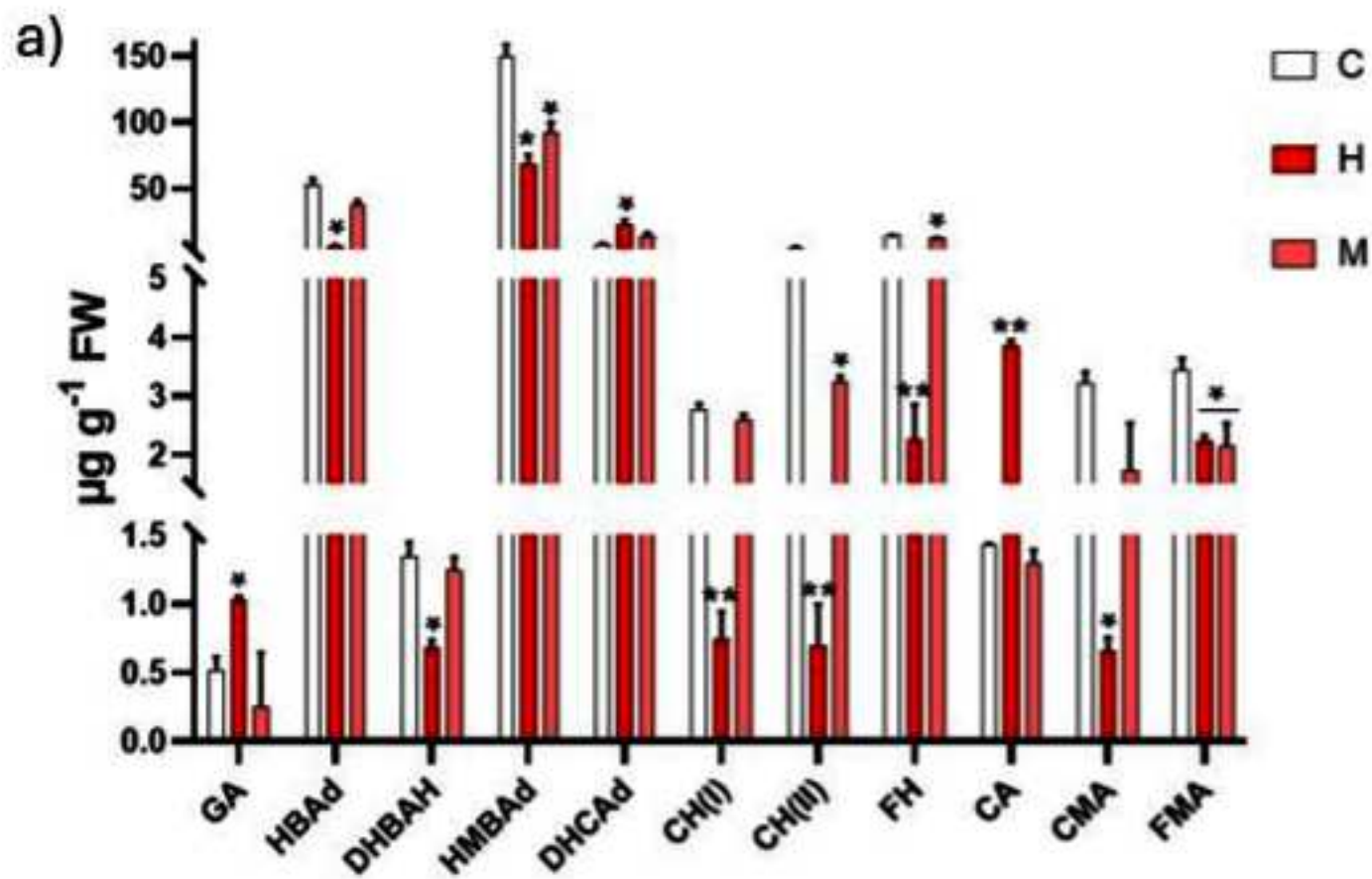
Table 1 (a) Activity of ascorbate peroxidase (APX), guaiacol peroxidase (POX), catalase (CAT) and superoxide dismutase (SOD) in rhizomes and leaves of *Cymodocea nodosa* plants exposed to different levels of seawater contamination by IBU (0 $\mu\text{g L}^{-1}$ or Ctrl, 0.25 $\mu\text{g L}^{-1}$ or Low, 2.5 $\mu\text{g L}^{-1}$ or Medium, 25 $\mu\text{g L}^{-1}$ or High), and (b) concentration of chlorophyll a (Chla), chlorophyll b (Chlb), total chlorophyll (Total Chl) and carotenoids in leaves of *Cymodocea nodosa* plants exposed to different levels of seawater contamination by IBU. Different letters denote significant differences ($p < 0.05$) among treatments.

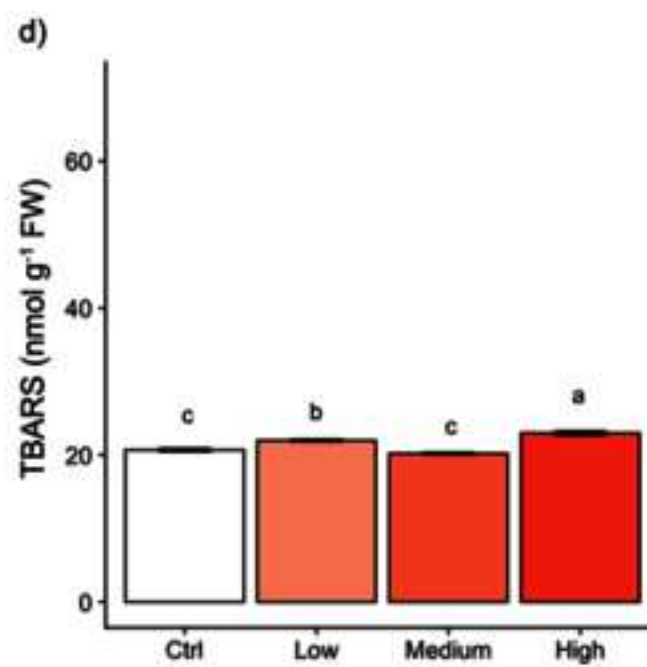
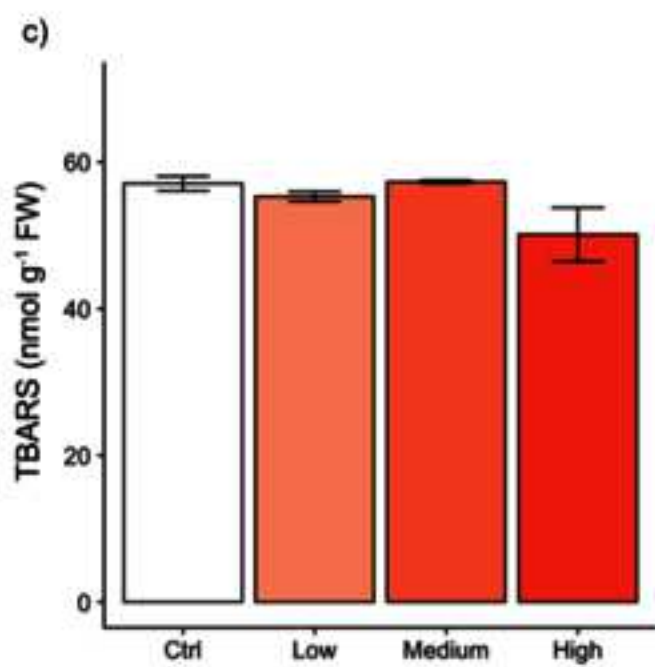
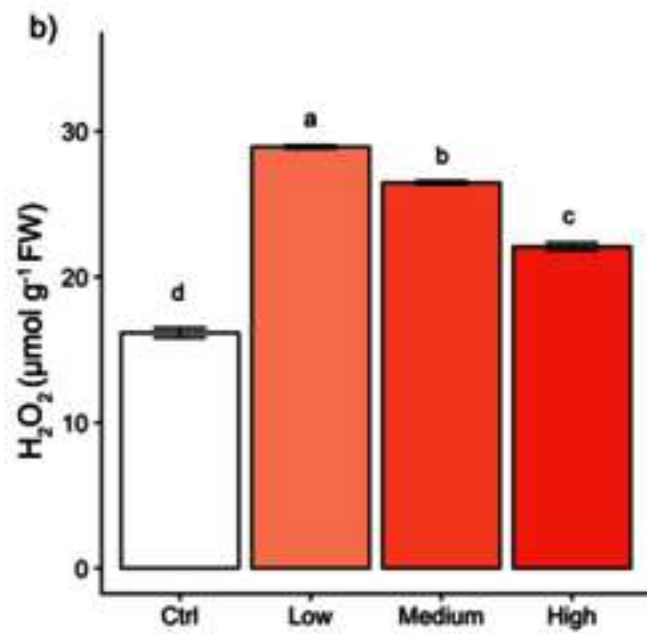
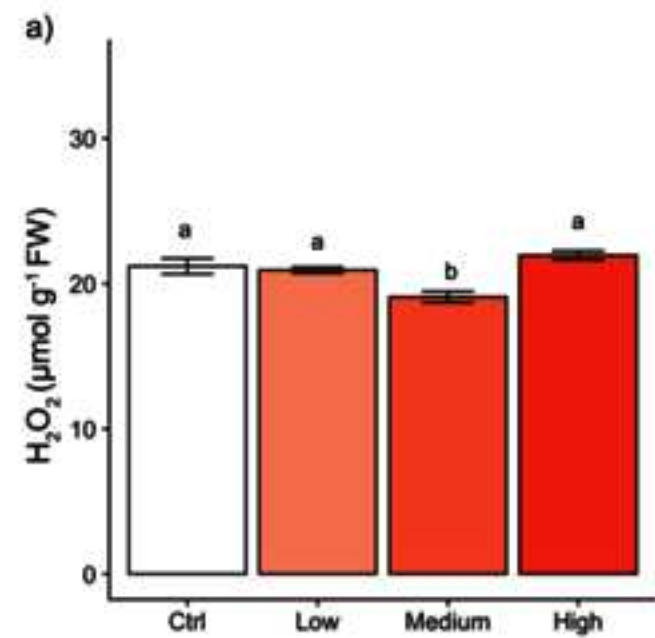
(a)	APX		POX		CAT		SOD	
	Rhizomes	Leaves	Rhizomes	Leaves	Rhizomes	Leaves	Rhizomes	Leaves
Ctrl	0.66±0.01 b	0.77±0.02 bc	5.50±0.30 a	5.38±0.29 b	2.44±0.24 ab	4.41±0.28 a	39.66±1.45 a	40.23±0.76 a
Low	0.90±0.08 ab	1.09±0.08 a	5.92±0.36 a	10.23±0.62 a	2.00±0.21 b	5.12±0.32 a	37.26±2.46 a	29.06±7.15 a
Medium	0.94±0.02 a	0.84±0.02 ab	4.98±0.53 ab	5.52±0.34 b	2.44±0.24 ab	4.08±0.34 a	33.96±4.66 a	40.80±1.42 a
High	0.66±0.01 b	0.67±0.03 c	3.37±0.06 b	3.26±0.32 c	3.02±0.14a	4.32±0.26 a	40.80±0.93 a	36.12±4.74 a

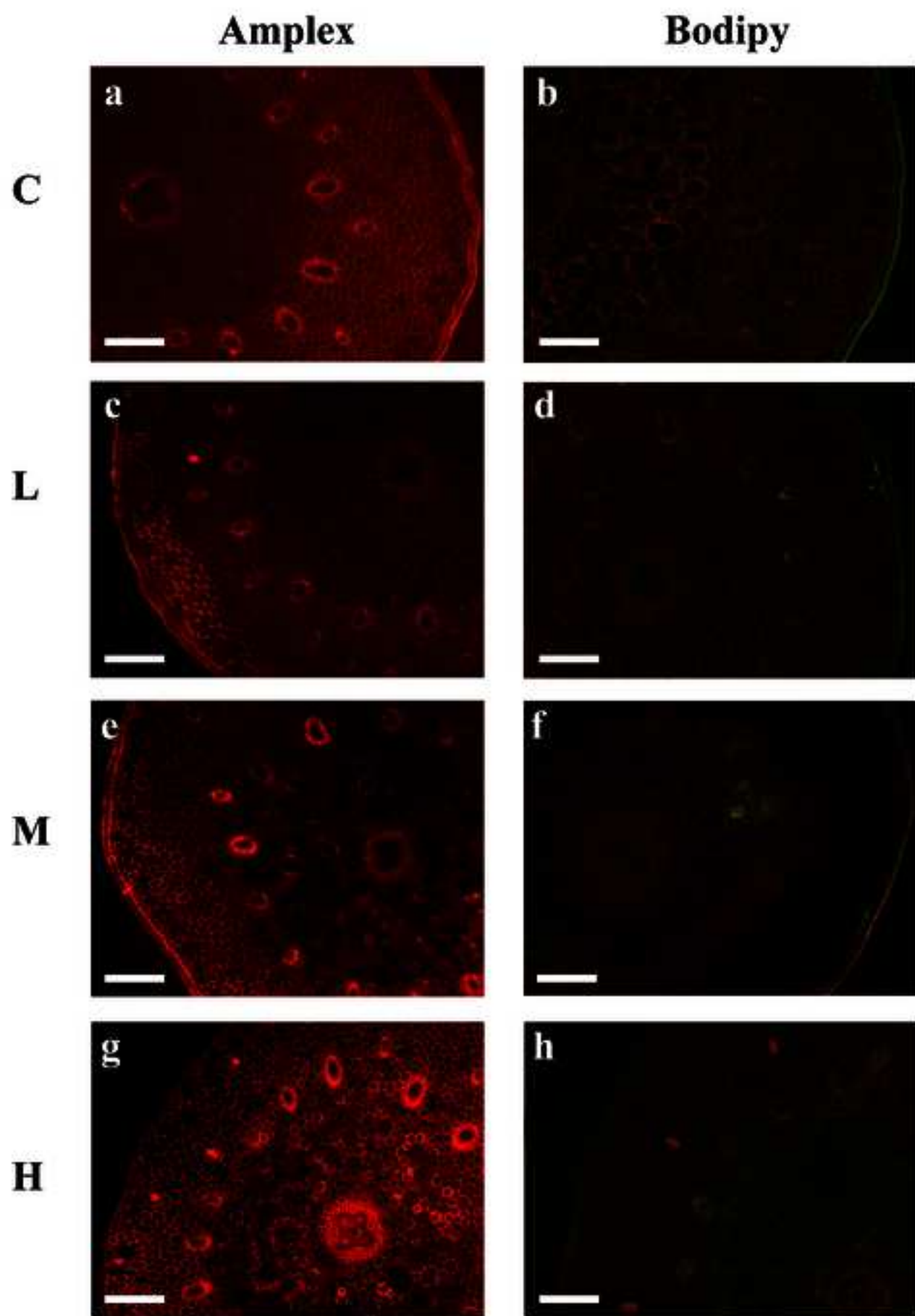
(b)	Chla	Chlb	Total Chl	Carotenoids
Ctrl	0.42±0.09a	0.27±0.05b	0.69±0.17b	0.10±0.01b
Low	0.38±0.04a	0.29±0.02b	0.67±0.07b	0.09±0.02b
Medium	0.50±0.07a	0.31±0.02b	0.81±0.11ab	0.15±0.02b
High	0.77±0.08a	0.50±0.02a	1.27±0.08a	0.22±0.00a

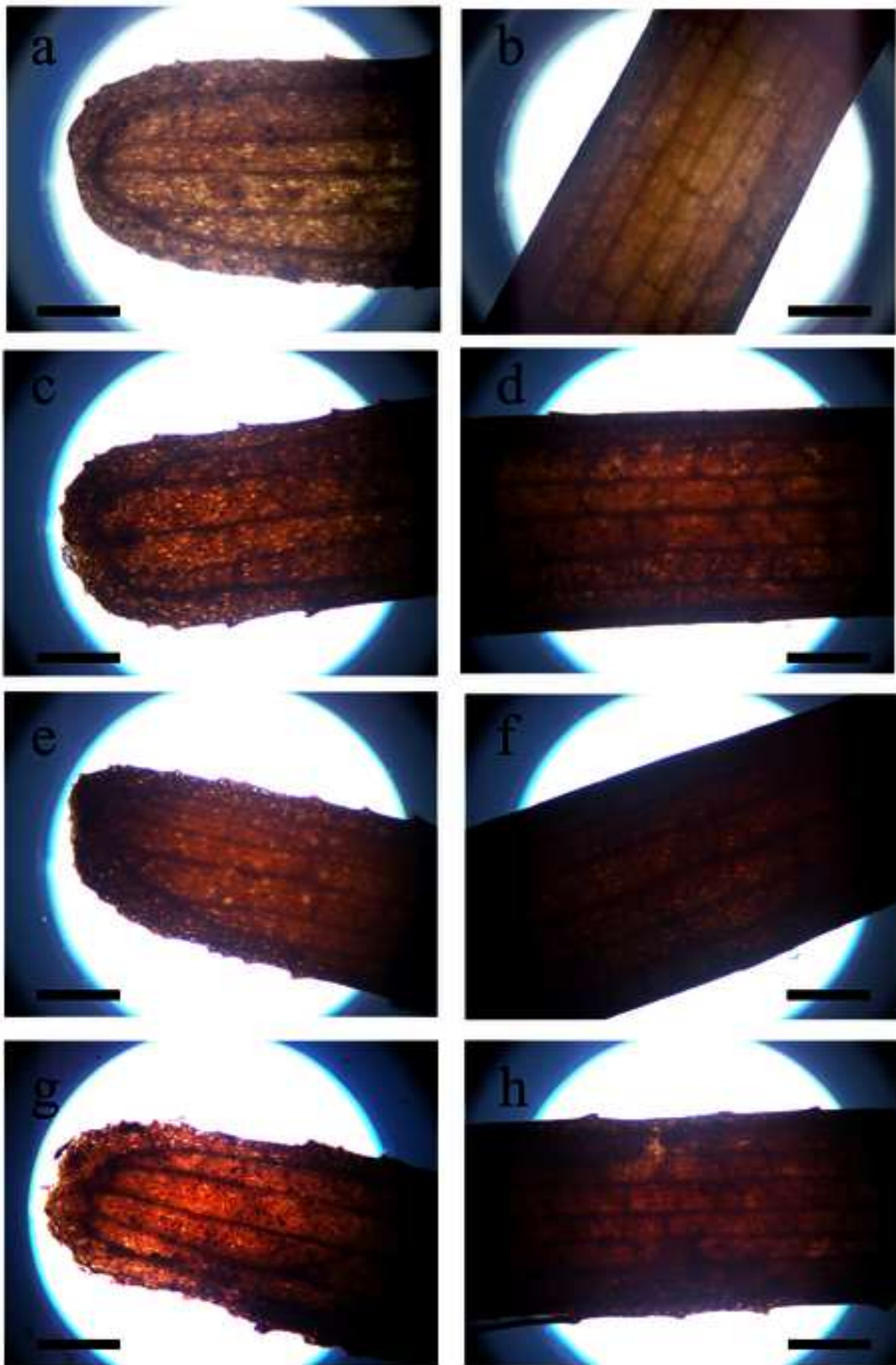


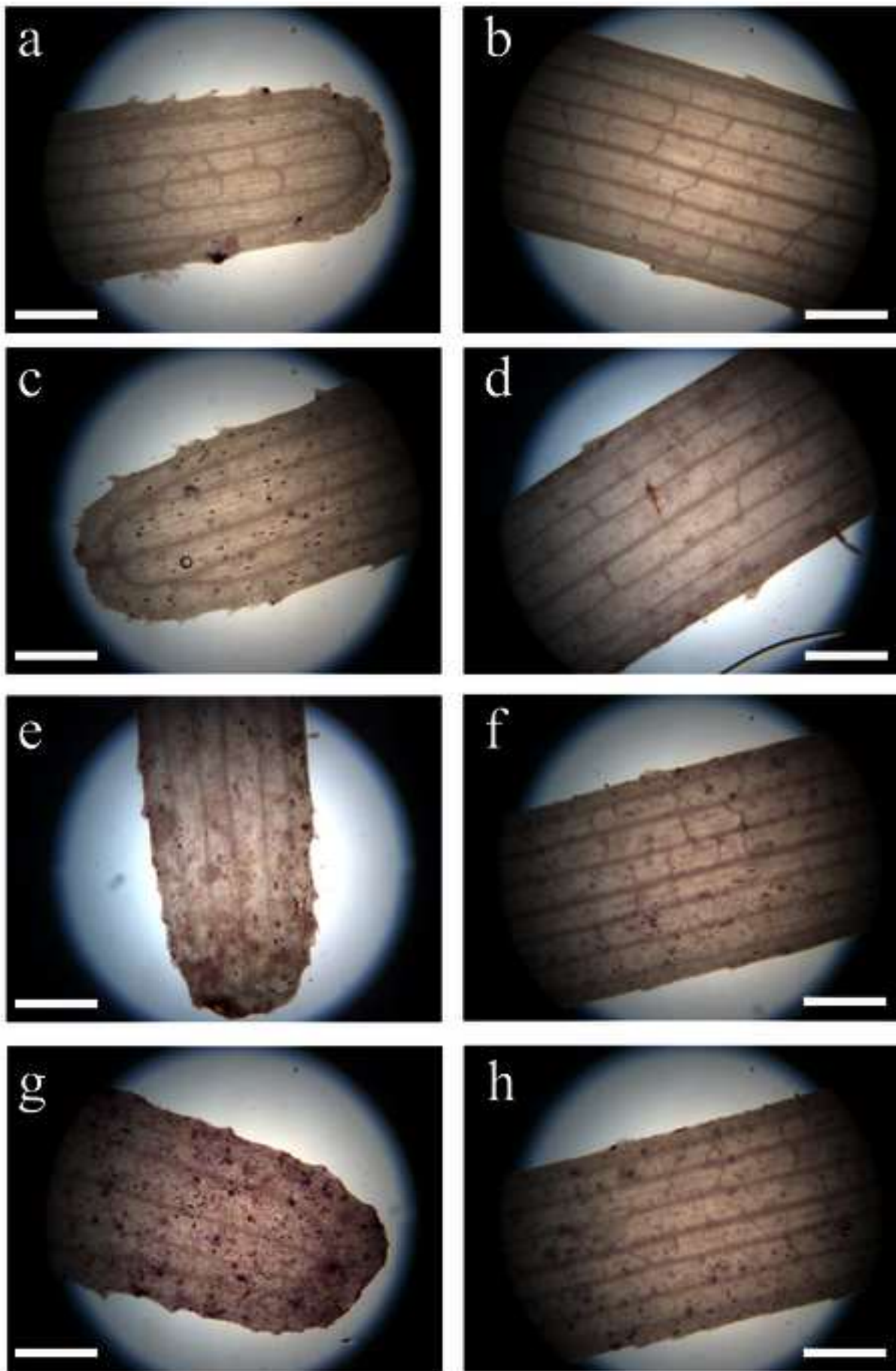


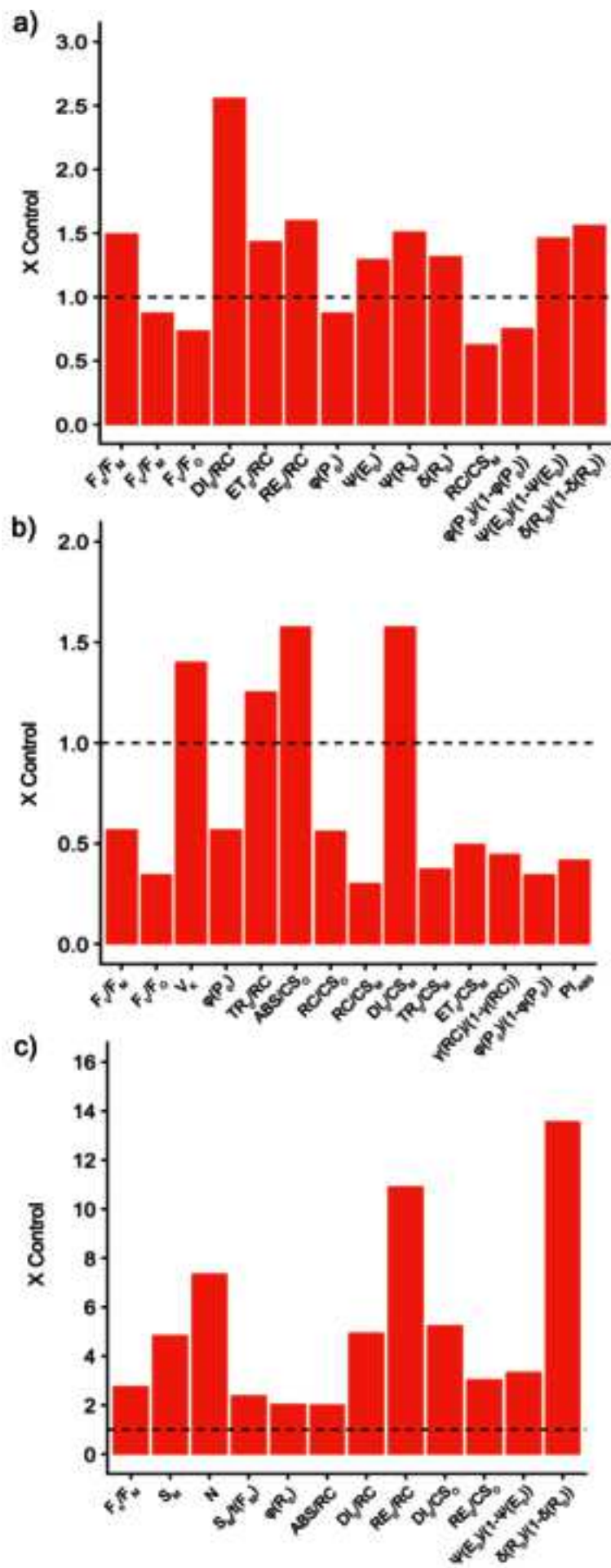














Click here to access/download
Supplementary Material
Supplementary Materials.docx



Declaration of interests

The authors declare that they have no known competing financial interests or personal relationships that could have appeared to influence the work reported in this paper.

The authors declare the following financial interests/personal relationships which may be considered as potential competing interests: